Droplet Impact on Supercooled Surfaces

BY

VIJAY PRITHIV BATHEY RAMESH BAPU
B.E., Anna University, 2014

THESIS

Submitted as partial fulfillment of the requirements for the degree of
Master of Science in Mechanical Engineering in the Graduate College of the
University of Illinois at Chicago, 2017

Chicago, Illinois

Defense Committee:

Sushant Anand, Chair and Advisor
Constantine M. Megaridis, Mechanical Engineering
Roberto Paoli, Mechanical Engineering

Acknowledgement

The journey as a graduate student has been a great learning experience but an enriching one. It has taught me the true meaning of the virtues of honesty, hard work and perseverance. I wish to take this opportunity to acknowledge the contributions of all those without whom this work would not have reached fruition. To begin with, I would like to thank my Master's thesis advisor, Prof. Sushant Anand for his unrelenting support during this work. His enthusiasm for science and easy accessibility was greatly beneficial in successful completion of this thesis. He has been more than a mentor to me, one without whom my graduate life would be anything but the smooth ride it turned out to be eventually. I gratefully acknowledge my Master's thesis committee members, Prof. Constantine Megaridis and Prof. Roberto Paoli for accepting to be on my committee and providing their valuable feedback. Next, I would like to thank Dr. Varun Kulkarni and Dr. Dongjin Kang for extending their help and support in solving critical issues during the experiments and data processing. I also place on record a special thanks to Mr. Eric Schmidt of the machine shop for all the technical support. Much of the experimental work would not have been possible without his help in fabrication. I thank my lab members for their cooperation at various stages of this thesis work

My family (mother, father, brother) has been a tremendous support despite the many miles that have separated us. Their constant encouragement and support has kept me going through the ups and downs of being an MS student. I am indeed blessed to be part of such a family and hope their good wishes remain with me forever. Lastly, there may be many whom I may have missed mentioning here, unknowingly or due to limitations of

this space but that in no way diminishes the gratitude I have for them. I extend a heartfelt thank you to them and for their contributions.

Vijay Prithiv Bathey Ramesh Bapu

University of Illinois at Chicago,

July 2017

List of Contents

List of Tables

List of Figures

Abstract

Dry ice, traditionally, has found tremendous application in food storage and blast cleaning. In recent years, there has been renewed interest in exploiting the sublimating vapor of dry ice as a liquid repellent for contactless transport thereby reducing drag. This work investigates the impact of a hexadecane drop on a sublimating layer of dry ice at room temperature. The sublimating CO_2 layer formed above the dry ice is compressed as the drop approaches the solid surface. Liquids which have lower specific heat capacity and latent heat comparatively can therefore freeze partially before bouncing at certain low Weber numbers. This unravels a hitherto unknown regime as current literature describes bouncing at low Weber numbers which is immediately followed by sticking and freezing at higher Weber for a given class of fluids. We thus examine the impact of a hexadecane drop below its capillary length on dry ice which exhibits this kind of behavior. The applicability of hexadecane as phase change material (PCM) also makes its use attractive in such a study. As the hexadecane drop spreads on this vapor cushion partial freezing ensures the movement of the contact line is arrested and we observe lower maximum drop spread (D_{max}) values *viz-à-viz* impact on Super hydrophobic or Leidenfrost drops which display similar behavior. Furthermore, the drop is acted upon by hydrodynamic instabilities which lead to formation of fingers which give rise to an interesting petal shaped pattern. Our study aims characteristics these various morphological transitions in this regime where there is partial freezing accompanied by bouncing and sticking depending on the impact Weber number. This research thus aims to further our knowledge of drop impact on dry ice with the view of helping us better understand development of

liquid repellant coatings and application where drag reductions is important.

CHAPTER 1

INTRODUCTION

In this chapter, we will discuss about basic physics of the droplet interaction with the surfaces and its importance followed by the wettability characteristics and contactless transport methods.

1.1 Droplet Interaction with the Surface

Studying the interaction of droplets with different types surfaces in very essential from the perspective of understanding the underlying Physics as well as the applications in the real world. There are numerous situations where we come across the liquid drop interaction with different types of surfaces (solid, liquid and sublimating). Some of the common applications are self-cleaning, spray coating, ink-jet printers, water repulsive coatings and water harvesting [1-5]. The characteristics of interaction between the droplet and surface depends on the properties of liquid drop, impacting velocity, substrate type, temperature of the substrate and the medium through which the drop progresses prior to the impact. It is necessary to understand that the collision dynamics of the liquid droplet can differ greatly for different type of surfaces [6]. Hence, it is very important to consider the droplet interaction with surfaces and their outcome before selecting a practical application. For example, in the spray painting application, the droplet must be able to adhere to the surface uniformly to coatings. In water harvesting application, the droplet must be capable of effectively rolling and falling into the reservoir without much sticking and loss in the total volume. Similarly, the liquid drops must be able to roll freely and

clean the dust particles off the surface in the self-cleaning technique. Figure 1.1 illustrates some of the applications of the droplet/ surface interaction applications.

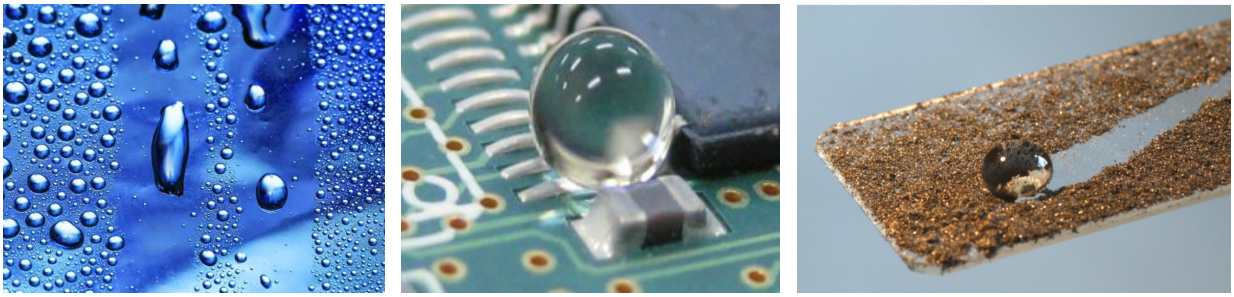

a *b* *c*

Fig 1.1 – Droplet and surface interaction applications – a) water harvesting, b) super hydrophobic coatings for electronics and c) Self-cleaning

Droplet and surface interactions can also be seen in nature in our day-to-day life. Taking nature as an inspiration, constant research is being carried out to bio-mimic these unique properties to obtain advance surfaces and structures. Some of the nature driven motivations can be traced in the superhydrophobicity of lotus leaves repelling water drops, the fogstand beetle *(Stenocara racilipes)* in the Namibian deserts have the capability of collecting water from condensing fog, rain drops impacting the earth etc. Figure 1.2 illustrates the droplet/ surface interactions that can be observed in nature.

Extensive research is being carried out in this field to understand the physics and mechanism governing the droplet impact process in the above-mentioned applications. Many theories and relationships have been put forward by various academicians that govern the droplet impact phenomenon which are reviewed in Chapter 2. The ultimate objective of this thesis is to test the interaction of an oil droplet over a sublimating substrate and validate the obtained results with the water droplet impact over the same substrate.

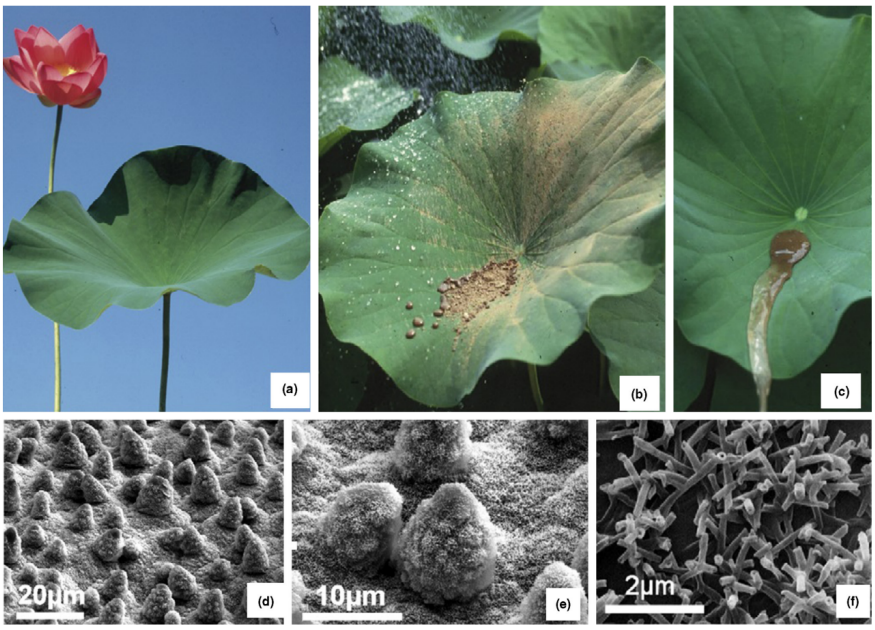

Fig 1.2 – Lotus leaf effect – droplet interaction in nature (adopted from [7])

1.2 Factors governing liquid droplet interaction with surfaces

The liquid droplet interaction with surfaces is mainly influenced by the below listed factors. They are as follows

a.) **Substrate properties:** The physical properties of the substrate include the surface quality (mean surface roughness), topography of the surface and the chemical properties include the nature of the surface (Wettability characteristics), temperature of the substrate, density and viscosity (for liquid or sublimating substrates) and rate of sublimation.

b.) **Liquid droplet characteristics:** This includes some of the parameters related to the physical quantities of the droplet like the sphericity, impact velocity (U_o) of the droplet, the height and time scale of the droplet fall.

c.) **Physical properties of the droplet:** These include the dynamic viscosity (μ), surface tension (σ), freezing point of the liquid (T_i), density (ρ)etc.

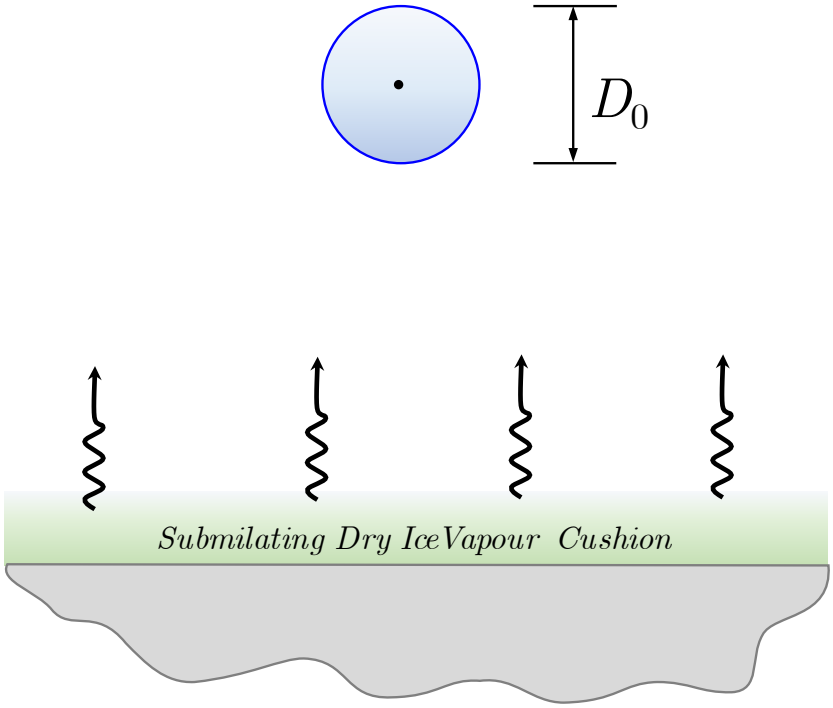

Fig 1.3 – Schematic illustrating the factors influencing droplet/ surface interaction.

1.3 Influence of Wettability of droplet interaction

Here, we will consider the details of the characteristics of wettability and how it affects the droplet interaction with the substrates.

1.3.1 Wettability and its characteristics

Wettability is defined as the ability of a fluid to spread over a solid surface and maintain contact with it. Degree of wettability of a liquid/ surface interaction is determined by the balance between the cohesive and the adhesive forces. Based on the degree of wettability the surfaces are classified as follows - *Super Hydrophilic, Hydrophilic,*

Hydrophobic and Super Hydrophobic surfaces. It is mainly characterized by the contact angle the droplet makes with the substrate. In other words, if a droplet spreads over the surface easily, it is said to exhibit hydrophilicity and if the droplet makes higher contact angle with the substrate, then it is said to exhibit hydrophobicity. Generally, a super hydrophilic surface has total wetting of liquid over its surface, while the super hydrophobic surface has the liquid droplet balancing over it with a very large contact angle (very small contact area with the surface) [8]. Table 1.1 compares the wettability to the contact angle of a liquid drop on a substrate and Figure 1.4 illustrates the contact angle made by the liquid droplets on different types of substrates with chemical properties.

Table 1.1 – Degree of Wettability for corresponding contact angles.

Wettability	**Contact Angle (θ)**
Perfect Wetting (or) Super Hydrophilicity	$\theta = 0^o$
High Wettability (or) Hydrophilicity	$0^o < \theta < 90^o$
Low Wettability (or) Hydrophobicity	$90^o < \theta < 150^o$
Perfectly non-Wetting (or) Super Hydrophobicity	$\theta = 180^o$

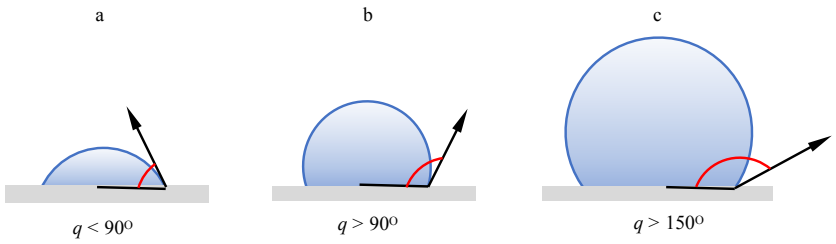

Fig 1.4 – Contact angle made by various substrates – a) Hydrophilic substrate, b) Hydrophobic Substrate and c) Super Hydrophobic Substrate

Apart from the chemical characteristics of the substrate, there is a physical parameter called surface roughness which plays an important role in cohesion and adhesion of liquid drops. This theory is explained by two models namely a) Casie-Baxter State and b) Wenzel State [8, 9].

Casie-Baxter State – This state arises when there is a solid substrate with a roughness factor in which air or ambient gas is trapped between the cavities. In this case, since there is a uniform cushion of air under the liquid droplet, it is still capable of sliding/ rolling over the substrate.

Wenzel State – This is the state in which the solid surface with a roughness factor with a droplet sitting over it fills the cavities. Here, adhesion of the droplet is observed. The Casie-Baxter and Wenzel State of a droplet, resting on a solid substrate can be referred in Figure 1.5.

However, in this work, we are dealing with a sublimating substrate that has a thin layer of sublimating gas that deviates from the above mentioned two states. This phenomenon will be discussed in detail in the forthcoming chapters.

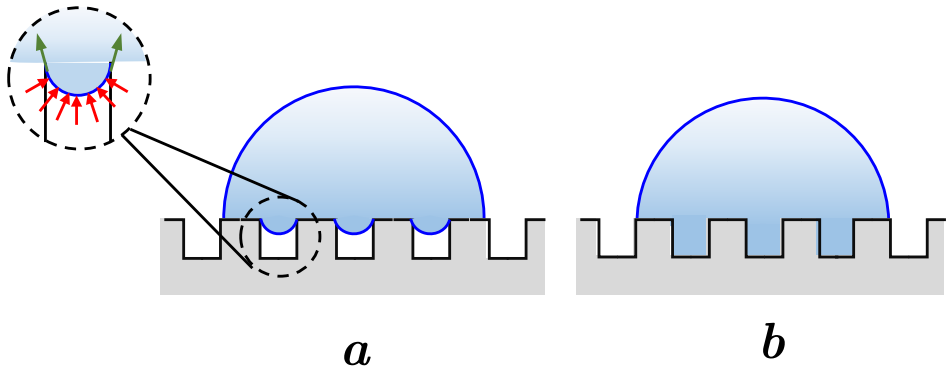

Fig 1.5 – Wetting models a) Casie-Baxter State and b) Wenzel State

1.3.2 Super Hydrophobic Surfaces

Super hydrophobicity is a phenomenon where the chemical properties and the surface roughness parameter are balanced in a proportion to generate a water-repellant surface. Generally, the wettability of these substrate is very low and the liquid tends to roll off or bounce away upon impact [10]. These surfaces are generally characterized over the other surfaces by the droplet contact angle while it is at rest over the substrate. The hydrophobicity is also a function of wettability and contact angle. Table 1.1 summarizes the characterization technique of surfaces.

Super hydrophobic surfaces have its advantages over normal surfaces depending upon the application it is used for. Super hydrophobic surfaces mainly find applications in water-repellant coatings, corrosion resistant coatings, water harvesting etc. as discussed previously. Super hydrophobic surfaces are preferred in places where the sticking of water to the surface in unnecessary. Sensitive metals are coated with super hydrophobic coatings and sprays so that water doesn't encounter the metal directly or stick to it causing oxidation and corrosion [11, 12]. In water harvesting, the surface must be super hydrophobic so that the collected water falls directly into the reservoir without sticking and loss in volume.

Super hydrophobic surfaces are known to reduce drag and friction in fluid systems. Friction Drag Reduction (FDR) properties can be found in super hydrophobic surfaces and hence it finds applications in many fields [13]. Drag creates unnecessary friction and sticking causing losses in volume, flow and velocity. It is mainly caused by the surface roughness present in the surfaces. It has been proved that the usage of super hydrophobic coatings can reduce drag in fluid systems by considerable amount leading to better

efficiency. Moreover, this drag reduction mechanism works fine for both laminar as well as turbulent flows [14]. There are several fabrication methods adopted to create hydrophobic and super hydrophobic surface structures. Some of the methods are lithography, chemical deposition, self-assembly of particles etc. Nanograss surface structure is illustrated in Figure 1.6.

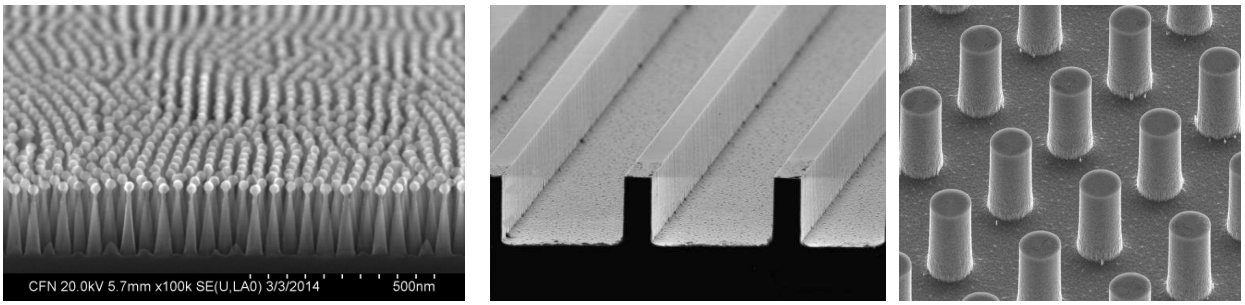

a *b* *c*

Fig 1.6 – Super hydrophobicity can be induced be the following surface structure modifications a) Nanograss surface structure, b) Nano ribs on Silicon wafers and c) Microscopic pillars on the Silicon wafers. (pictures adapted from https://phys.org/news/2014-05-super-waterproof-surfaces-ball.html)

Though there are several methods to chemically modify surfaces and obtain super hydrophobicity, all these methods are time consuming and expensive processes [15]. A good level of skills is required to fabricate these surface structures precisely and accurately. To overcome this, there are spray coatings that induce super hydrophobic properties to the substrates. These sprays mostly contain Hydrophobically Modified Silica (HMS) particles in polymer emulsions. Hydrophobic sprays are generally easy to use and the wait time to obtain a modified surface is very less compared to previously fabricated techniques. However, the durability of these coatings is a question mark. Strong, durable suspensions are being tested to make coatings that last for longer duration without loss in its properties. Some of the commonly available spray coatings in market are *NeverWet*

by RUST-OLEUM, Hydro-Lok by RAIN GUARD etc. They are commonly used for daily life applications to incorporate anti-wetting, anti-corrosion, anti-icing and self-cleaning properties.

Fig 1.7 – Applications of the super hydrophobic sprays and coatings in daily life. Treated surface represents the spray coating in effect and the un-treated surface is the default surface.

Super hydrophobicity, in the above cases are all obtained by making chemical modifications in the material and/ or surface topology. But there is a non-contact method that can induce temporary hydrophobicity on normal solid surfaces. It is called non-contact because, the liquid droplet doesn't meet the surface of the substrate. Instead, it is rebounded by a thin layer of fluid cushion forming an interface between the droplet and the substrate. The fluid may be air, ambient gas or impregnated liquid layer in the substrate itself. A low thermal conductivity fluid flow in the solid-liquid interface will reduce the heat transfer characteristics. This enable the drop to rebound or hover over the substrate upon impact, without touching the substrate for moderate velocities [16, 17]. However, the fluid film breakdown occurs when the drop velocity is high, leading to sticking/ splashing regime of liquid drops [18]. Similar film breakdowns can also be related to the bag formation of jets falling in an air stream. It is clear that the droplet impact

phenomenon also has resemblance to other impact phenomena such as drop impact by a stream of fast flowing air [19, 20]. Contactless rebound on solid Carbon dioxide (dry ice) is one such good example of droplet impact on supercooled substrates. In the upcoming chapters, dry ice as an Oleophobic and super hydrophobic substrate for Hexadecane and water droplet impact will be discussed in detail. To sum up, super hydrophobicity achieved by contactless method is more advantageous and superior compared to conventional methods because of the versatility, contamination free method and time required to treat is very low.

1.3.3 Contactless Transport

Usually when a liquid drop impacts on a solid substrate, it encounters the surface before it bounces away. However, in certain cases this may not be trued. There is a thin layer of ambient gas at the interface that causes the droplet to bounce without even touching the substrate – reported as droplet levitation phenomenon in solid Carbon dioxide (CO_2) [21]. There are three cases where this effect can be observed –

- Leidenfrost Effect
- Induced Air cushion interfaces
- Sublimating substrates

1. Leidenfrost Effect

Leidenfrost effect is a phenomenon where the liquid, when in near contact with a substrate at significantly hotter temperature than the boiling point of the liquid, produces a vapor layer that acts as an insulation keeping the liquid from rapid boiling. This vapor layer acts as a cushion, creating a repulsion between the substrate and the droplet. Hence,

we observe the droplet doesn't come in direct contact with the surface and hovers over it. This phenomenon can be commonly observed in hot cooking pans when water is sprinkled [22]. In a dangerous trick that involves dipping the hand into molten lead involves Leidenfrost effect too. Initially, the hand is prepared by dipping into cold water so that dipping the hand in molten lead evaporates the layer of water, producing a thermal insulating vapor layer around the hand [23, 24]. Figure 1.8 demonstrates the Leidenfrost Effect on hot substrates. Leidenfrost effect can be observed typically when the temperature of the substrate is greater than 200 °C [25].

2. Air Cushion Droplet Hovering

Like the Leidenfrost effect, air cushioning is a phenomenon where a thin film of air is passed over the substrate to achieve contactless rebound of liquid droplets. The air layer plays a very critical role in the drop wetting properties. This effect was first observed in vibrating liquid surfaces and in Leidenfrost droplets with vapor layer [26]. The air cushion is broken for a few fractions of a second when the impact velocities are high, causing the droplet to penetrate the layer. However, for moderate impact velocities, the air layer is intact and squeezes in and out gentle upon impact, causing drops to rebound. Also, the film thickness is a function of the weber number, which means that the squeezing layer thickness constantly changed for drops impacting from different heights during the spreading over the film [27, 28].

3. Sublimating Surface

Sublimation is the process of conversion of a solid substance into gaseous state without undergoing liquid phase transition. This is said to happen when the process pressure and temperature is below the triple point of the substance in the Phase diagram.

Some good examples of sublimating materials are solid Carbon dioxide (dry ice), Camphor, Napthalene and Iodine. When these materials sublimate, there is a thin layer of vapor layer of white smoke above the surface which acts as a thermal insulator. Drop impact on sublimating surfaces (dry ice) is comparable with the Leidenfrost effect because of the presence of a vapor layer that acts as a thermal insulation due to substantial temperature gradient between the liquid droplet and the substrate [26]. Dry ice substrate is used for the study of hexadecane and water droplet impact test in this work because of the exceptional super hydrophobic as well as Oleophobic properties to a large variety of organic oils and chemicals. The naturally present sublimating layer in the dry ice is responsible for the rebound and hovering of droplets without sticking to the surface [21]. Also, most of the solid substrates lose its Super hydrophobicity at low temperatures due to the formation of frost leading to increase in ice adhesion, which questions the reliability at low temperatures. This alteration in wettability with change in temperature is attributed towards the change from Casie-Baxter State to the Wenzel State [29, 30]. Dry ice can be an exceptional replacement of solid substrates for low temperature surface applications which is discuss in this work. Figure 1.9 demonstrates the contactless bouncing of liquid drop on the sublimating layer of dry ice.

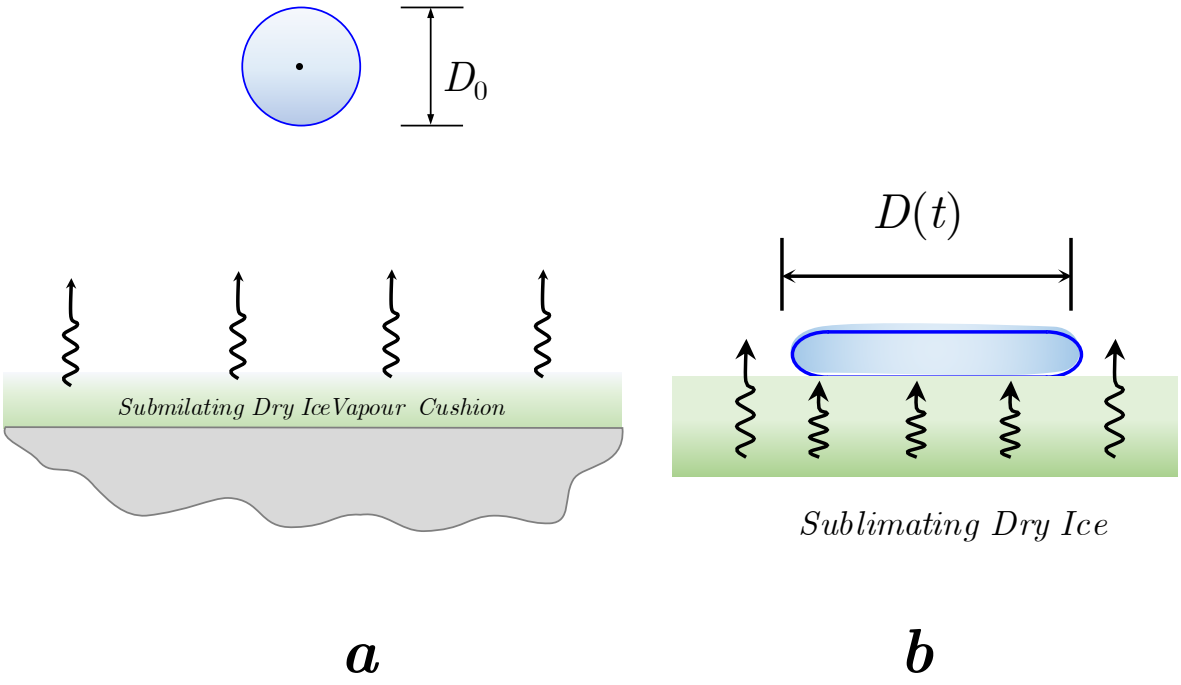

Fig 1.8 – a) Droplet of initial diameter D_o approaching dry ice vapor cushion, b) Droplet spreading on the vapor cushion. D(t) represents the dynamic change in drop diameter with time on spreading.

1.4 Motivation and Objective behind the study

Droplet-surface interaction is encountered in several engineering applications in day-to-day life events. It is very mandatory to study and control the drop impact phenomenon by manipulation. Some of the familiar applications in the above context are spray painting of Body in White (BIW) in automotive industries, Water harvesting, ink-jet printers and self-cleaning surfaces. In case of spray painting, it must be ensured that the pain sticks to the surface and forms a uniform coating over it. On the contrary, splashing of ink on paper material is highly undesired in printing [1]. To achieve control over the droplet-surface interaction it is very necessary to understand the physics behind the droplet impact process and the relationship between different physical parameters

related to the liquid and the surface. In this work, dry ice as a super hydrophobic and Oleophobic substrate has been investigated for the drop impact process with n-Hexadecane and validated the results with that of water. So far, in the literatures, there are evidences about two regimes namely – Drop rebound and Drop splashing. In the present work, a completely new regime has been uncovered for liquid with low surface tension, latent heat and high melting point.

The present work deals with a droplet interacting with a sublimating substrate from different heights. It is said that the spreading factor is a function of weber number and it is a universal value for all kind of substrates [26]. To check and validate this, experiments will be performed to fulfill the following objectives.

1. **The spreading diameter of the drop is an important parameter that helps us in determining various parameters like the spreading velocity and the retracting velocity.**
2. **Maximum diameter of the droplet after impact for each a given Weber number increases with height. This parameter will help, design a system for a given application.**
3. **Contact time of the droplet helps in the study of the characteristics of the drop to stay in contact with surface from the moment it impacts till the departure. When there is larger contact time, it is an indication of larger spreading.**
4. **The rebound velocity is an important parameter that is justified and explained by the contact time of the droplet and the Rayleigh time of the fluid.**

5. **Number of Fingers/ Petals for the given Weber number is important to study the splash characteristics of the droplet falling from different heights.** (splashing in undesirable in ink-jet printing, while fine fragmentation is necessary in fuel spray injectors in the engine combustion chambers.)

1.5 Thesis Layout

The workflow of the thesis is organized as follows. The present chapter, Introduction, considered the droplet interaction with surfaces giving a wide picture about the physics behind droplet impact and the factors governing this phenomenon. The advantages of the contactless transport method were discussed and finally the motivation behind the present study along with the main objectives were outlined. Chapter 2 gives a detailed review on the overview of drop impact morphology, contact time, non-dimensional numbers, impact of Weber number, instabilities and about the dry ice substrate. Chapter 3 explains in detail, the properties of the test liquids and the substrate, the experimental setup used and methodology followed to perform, obtain and process the results. The discussion also includes the measurements involved with drop impact such as the Sphericity of the droplet and comparison of the theoretical to experimental impact velocity. Chapter 4 presents the findings of this thesis and the theories involved in the phenomenon taking place during the droplet impact process. From the present experimental investigation, several findings have been revealed and the highlights of the finding have been presented along with improvements and suggestions for the work to be carried out in the future in Chapter 5.

CHAPTER 2

LITERATURE REVIEW

This chapter provides a detailed review on the state of art literature relating to the current experimental investigation. This section is organized under three main parts: Overview of the drop impact studies, which covers the the wettability properties and characteristics of the substrates, criteria for bouncing and sticking, significance of contact time and about the non-dimensional numbers *(We, Re, Oh)* followed by the impact at higher Weber numbers on droplet spreading dynamics and instabilities induced in the system. Finally, the effects and impact of dry ice substrate in droplet rebound and literatures on it are discussed.

2.1 Overview of the Droplet Impact studies.

Droplet impact studies involves some complex physics and deep understanding in fluid dynamics. The process of liquid drop interaction with surfaces can be a complex phenomenon involving several controlling parameters like the drop morphology during fall, impact, spreading, retracting and bouncing. Each of the mentioned parameter can have unique influences on the droplet impact process leading and hence, studying the drop morphology is very necessary.

When a large drop falls from a height, it is subjected to gravitational force which may result in slight changes in the Sphericity of the droplet falling in free air. The common myth that falling rain drops take the shape of tear drops was disproved by Flower (1927) to show that it takes the form of butterfly wings due to some aerodynamics related to the

falling droplet in air medium [31, 32]. The average change in the shape of the falling raindrops were studied using radar echo technique and spotted irregularities [33]. Small droplets maintained spherical shapes (fog drops and water vapor in clouds) while falling rain drops were manipulated to changes in its geometry and the reason for this was unknown. It was justified that large drops had flow of air around it and the boundary layer streamlines curved till they finally separated creating a turbulent layer above the drop. This resulted in flattened bottom and smoothly rounded top surface of the drops [34, 35]. Lac et al., presented a work demonstrating the elongation of droplets while passing through different capillary diameters [36]. The drop size oscillation was otherwise referred to as creeping motion caused due to a gravity parameter called capillary length. There is a direct dependence of Capillary number and Deborah number in the perturbation of droplets. Drop diameters exceeding the capillary number experienced more perturbation due to higher separation in the streamline of the air [37].

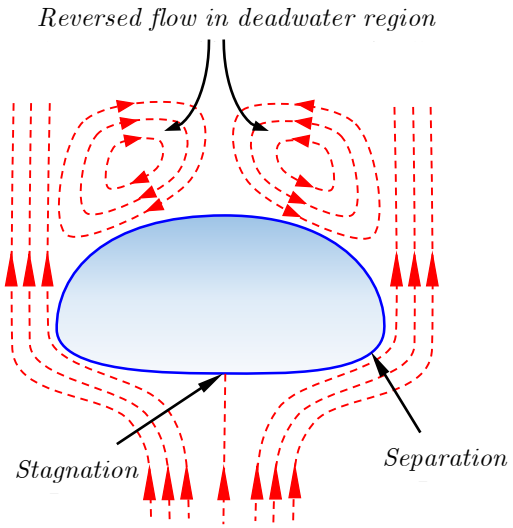

Fig 2.1 – Mean flow path of air responsible for the flattening of freefalling large drop at the bottom. Adapted from [34]

Flower (1928) mentioned about the effect of terminal velocity on the drop shape morphology. Larger drops accelerating at faster rates create more streamline separation leading to higher turbulence on the top side of the droplet [31].

Young (1805), laid the foundation for the droplet interaction with a solid surface and derived the relationship between equilibrium contact angle (θ) and the interfacial tensions (γ) at the respective interfaces (Solid-Liquid, Solid-Vapor and Liquid-Vapor) [38].

$$\cos\theta = \frac{\gamma_{SV} - \gamma_{SL}}{\gamma_{LV}}$$

Generally, the drop impact on surfaces is classified in regimes based on the characteristics exhibited by the drop after it had impacted on the surfaces. There are two regimes namely drop rebound or bouncing and drop splashing. The rebound and splashing criteria is decided by factors such as surface tension (σ), dynamic viscosity (μ), density of the fluid, impact velocity etc. Surface tension and impact velocity plays a huge role in deciding the rebound and splashing of impacted droplets [39].

The parameters mentioned above must be dimensionless so that it become easier to compare and evaluate. Some of the commonly used dimensionless sets related to drop impact are Reynold's Number *(Re)*, Weber Number *(We)*, Ohnisorge Number *(Oh)* and the Bond Number *(Bo)* (when there is gravity into effect) [40].

$$\mathrm{We} = \frac{\rho \mathrm{D} \mathrm{V}_o^2}{\sigma} \qquad \mathrm{Re} = \frac{\rho \mathrm{D} \mathrm{V}_o}{\mu} \qquad Oh = \frac{\sqrt{We}}{\mathrm{Re}} \qquad Bo = \frac{\rho g D^2}{\sigma}$$

It is important to have dimensionless parameters because it reduces the complexity of the problem and rounding-off errors. Using a dimensionless number, many dimensional parameters can be described is what makes it advantageous.

Sticking time or the contact time is another important parameter that helps determine the time until which the drop is in contact with the surface before bouncing off [41]. This parameter is important to determine the wetting characteristics of surfaces.

2.2 Impact of Low and High Weber Numbers

Worthington (1908) has investigated several drop impact experimental parameters in his book. The drop impacting a surface can either fall on a vertical trajectory or at an angle. Both will result in some interesting outcomes different from one another [42]. With increasing heights and velocities, expressed in the non-dimensional form, there are some interesting regimes and effects observed in the entire impact process discussed below.

2.2.1 Impact Morphology

The impact of the droplet with the surface results in spreading, retracting, bouncing and crater formation of the droplets [43]. Crater formation is an interesting phenomenon which can be observed in soft surfaces upon drop impacts. Craters created by liquid drops follow the same energy scaling as that of asteroid impacts in moon and mars [44]. This parameter is necessary to understand the effects of granular scattering leading to soil erosion by impacting drops. The study of force measurements revealed that the there was a peak pressure followed by rapid drop when compared to the force curves which is explained by the increasing surface area in contact with the surface [45]. The impact crater morphology is close to spherical in shape and the depth is a function of impact velocity and the striking angle.

2.2.2 Impact Regimes and Spreading Dynamics

When a drop impacts, it is accompanied by bouncing back (at low impact heights), spreading/ sticking (at moderate to high heights) and drop fragmentation (at high impact heights). Drop rebound was observed during the interaction with super hydrophobic surfaces at low impact velocities. This is attributed to the Casie-Baxter State, discussed in Chapter 1, due to the presence of air in the cavities [9]. The air layer entrapped under the droplet acts as a cushion, enabling rebound of the droplets. When the impact velocity is high, a change from Casie-Baxter state to Wenzel state is observed which leads to sticking of droplets on the surface [8, 46, 47]. The rebound time on super hydrophobic surface was found out to be a function of liquid droplet mass (m) and the surface tension (σ) rather than impact velocity [48]

Impact of droplet can lead to splashing when the impact velocity of the droplet greater than the experimental threshold velocity (V_{0S}), spreading of the drop is observed. When the threshold velocity is higher than the impact velocity, splashing and crown (petal) formation is observed because. At very large threshold velocity ratios ($V_{0S} >> V_{imp}$), the surface tension of the drop is completely overcome leading to fragmentation and formation of satellite droplets [49].

$$V_{0S} = 18\left(\frac{\sigma}{\rho}\right)^{\frac{1}{4}} \nu^{\frac{1}{8}} f^{\frac{3}{8}}$$

where - σ surface tension of the liquid-air interface, ρ - density of the fluid, μ - dynamic viscosity and f – frequency.

Apart from the plain rebound and splashing regime, there are classifications based on the type of bouncing, splashing and wetting properties during the drop impact – Deposition, prompt splash, receding breakup, Partial rebound.

The deposition is the scenario in which the droplet impacts and spreads over the surface completely and wets it without any splash or fragmentation. It is reported that, it takes place in two stages namely, Kinematic deposition and actual deposition [40, 50].

The prompt splash regime is observed when the impact velocity is high resulting in moderate Weber numbers causing detachment of tiny droplets from the lamella of the spreading droplet [40].

The partial rebound is a situation which can be observed in a liquid drop impacting from low weber numbers. Here, a part of the liquid sticks to the substrate while shooting one or two tiny droplets into the air due to capillary instabilities. For this to take place, there must be a large temperature gradient between the drop and the surface – molten drop deposition over a relatively cooler substrate [51].

Receding break-up is again a phenomenon observed when the relative temperature gradient between the drop and the surface is large. There is simultaneous sticking of drop accompanied by R-T instabilities causing petal growth which retract in a claw-folding manner [40, 52]. Presence of capillary instability may lead to further breakup of the petals. Some surface energy and the kinetic energy is conserved in the lamella region facilitating some retraction after the spreading has come to a stop. It is observed in mostly in a highly non-wettable surface [53]

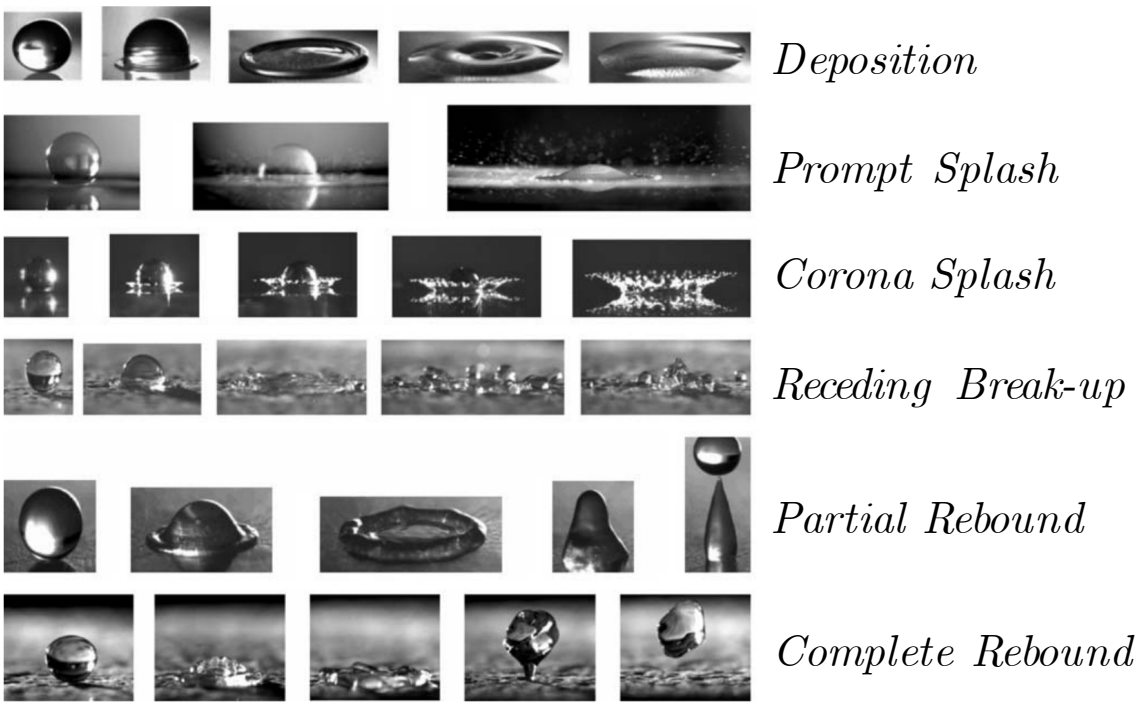

Fig 2.2 – Different drop impact dynamics of water summarized by Prof. Yarin in [40]

It is important to understand mechanism the spreading of the droplet when it impacts on a surface. At low impact velocities, the spreading is uniform, meaning, the thickness of the spreading is almost constant throughout the diameter. Whereas, in high velocity cases, there is a thinning of the center observed. The thinning at center is compensated by a thick rim is shown in Fig 2.2. The surface tension plays a very important role in hold the liquid molecules together. When the velocity is high enough to overcome the surface tension, the central region becomes too thin to hold the thick rim leading to fragmentation of the drop into satellite droplets [49, 52, 54, 55]. The drop receding mechanics is very same as that of the spreading mechanics and highly dependent on the surface tension of the liquid and the spreading velocity. The splat height was determined directly proportional to the impact velocity and the spreading of the drop was

a function of drop contact angle. Splat diameter reduced with reducing dynamic contact angle of the rim [56]. The momentum balance of the droplet receding mechanism was demonstrated as a factor of the inertial forces in the lamella after the velocity of the rim has come to a halt and but the lamella continues to move [52].

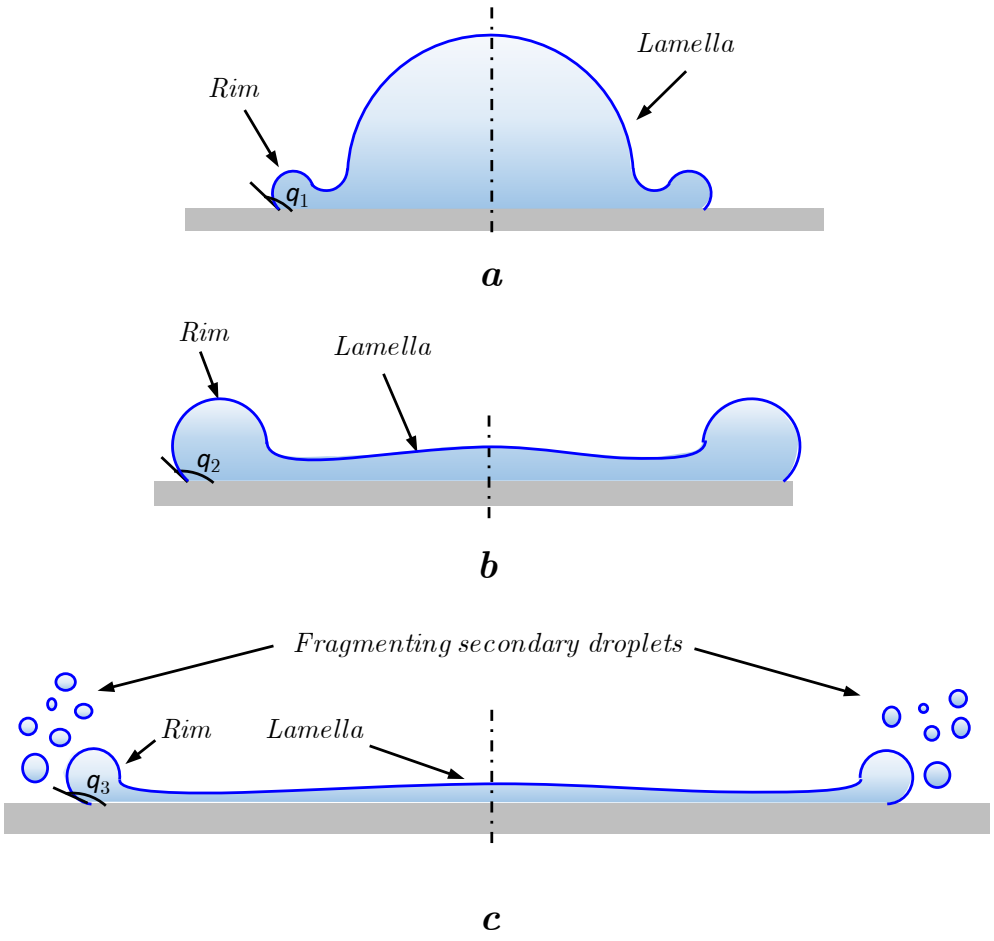

Fig 2.3 – Spreading dynamics of the droplet a) initial impact b) when spreading begins, thick rim and thin lamell and c) thinning of lamella followed by formation of secondary droplets.

2.3 Role of Instabilities

There are three instabilities that are commonly dealt with drop impact over surfaces – Kelvin-Helmontz (K-H) Instability, Rayleigh-Taylor (R-T) Instability and Capillary Instability. The K-H and R-T instabilities are two theories debated over the formation of petals while, the Capillary instability is responsible for the fragmentation of droplets into satellite drops after impact [40]. It is necessary to understand the basic difference between the two instabilities (K-H and R-T) first. K-H occurs when there is a velocity shear at an interface of two fluids causing wavy patterns on the surface of the fluid. R-T instability occurs when there in a rapid mixing of two a denser fluid into a less denser fluid, where the interface acts as a membrane. Figure 2.3 illustrates the two instability mechanisms.

Experimental observations of the effects of droplet velocity, density of ambient gas on the droplet were carried out to study their impact on droplet splashing. For a Weber number at very high range of 695 to 1800, velocity plays a dominant role with the ambient gas around the drop. The high velocity shearing the layer of ambient gas has resulted in empirical results matching that of K-H Instability during the splash of the droplet [57].

The formation of the fingering pattern during the splashing was correlated with the resistance created by the surface it is impacting upon. The thin layer of air entrapment under the droplet belly is the key factor leading to R-T instability [58]. The relationship between the number of fingers (N_f) formed with respect to the Weber number was formulated as follows,

$$N_f = 1.14We^{0.5}$$

This relation correlated universally to most of the liquids impacting on the solid surfaces [59]. However, this relationship has been disproved for sublimating surfaces in the present work and will be discuss in the upcoming chapters.

Capillary instability is related to the breaking down of drop into satellite droplets. It mainly occurs when the rim/ lamella ratio becomes too large and the inertia in the lamella exceeds that of the rim. The surface tension is overcome by the capillary forces leading to separation of the rim at various points from the lamella leading to detachment of sister droplets [60]. Mostly observed at high Weber numbers impacts as this instability is directly related to the V_{0S}/ V_{imp} ratio as discussed earlier in [49].

To conclude, Capillary instability is present naturally when the impact Weber number is large. However, the debate continues the R-T and K-H instabilities during the splashing regime. From the literature, it is quite convincing that the K-H instability is dominant when the Weber number range is large. In this present work, the Weber number range is well inside the range where R-T instability is dominant due to drops experiencing lower impact velocities.

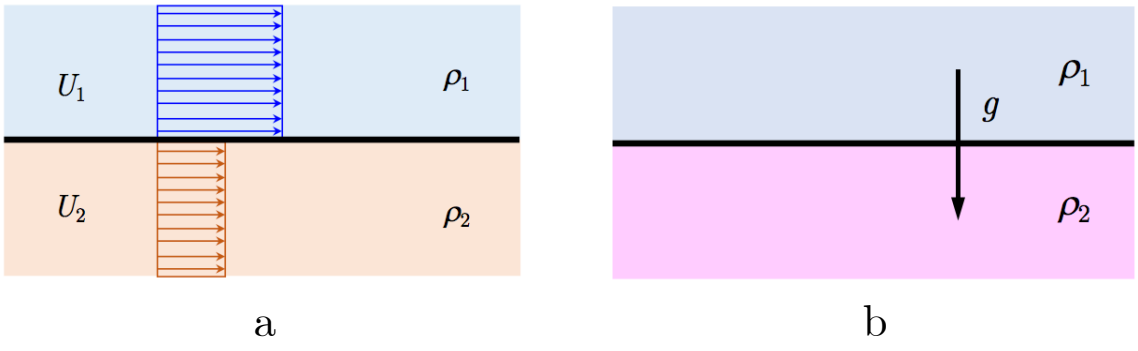

Fig 2.4 – a) Kelvin-Helmontz instability (density of ρ1 < ρ2) and b) Rayleigh-Taylor instability (density of ρ1>ρ2)

2.4 Dry Ice Impact

Solid Carbon dioxide (commonly known as dry ice), is a very interesting material exhibiting both Super hydrophobicity and Oleophobicity. The drop bouncing was related to two mechanisms – super hydrophobicity and Leidenfrost effect. Super hydrophobicity can be observed in low surface energy substrates and can be achieved by surface modifications, functionalization and inducing gas layers above the substrate.

Chemically modifying the surface structures and was first reported in 1950 [48, 60]. The Leidenfrost effect causes drop rebound when the liquid drop meets a superheated surface. A thin vapor layer is created by evaporation of the droplet which acts as a cushion – which was discussed in detail in Chapter 1 [25].

Dry ice is a sublimating material which has a visible layer of carbon dioxide over its surface. This sublimating gas, induces super hydrophobicity and is directly comparable to the Leidenfrost drops [29, 61]. In the Leidenfrost drop, the drop and the substrate are at a comparatively high temperature gradient which causes the drop to evaporate. Here, the dry ice is at much lower temperature compared to the liquid hexadecane drop and has a sublimating layer of gas (like the evaporating vapor layer in Leidenfrost drops). SHS, Leidenfrost and supercooled substrates has been widely studied and established for the bouncing regime of liquid drops. However, the sticking regime of liquid drops has not been investigated by many on the supercooled substrates.

In this work, we present the experimental observations on the petal formation (splash) regime for high velocity droplet impact on supercooled substrate (dry ice) and rebound regime for n-Hexadecane. A completely new regime was uncovered during the research called – Droplet "*freezing and bouncing*" – caused due to low high point and low

latent heat of the test liquid. The results deviate with the present literatures and to validate, test was also done for water drops impacting on dry ice. The detailed reasoning and discussion for *"freezing and bouncing"* phenomenon and the finger formation due to instability are presented in Chapter 4.

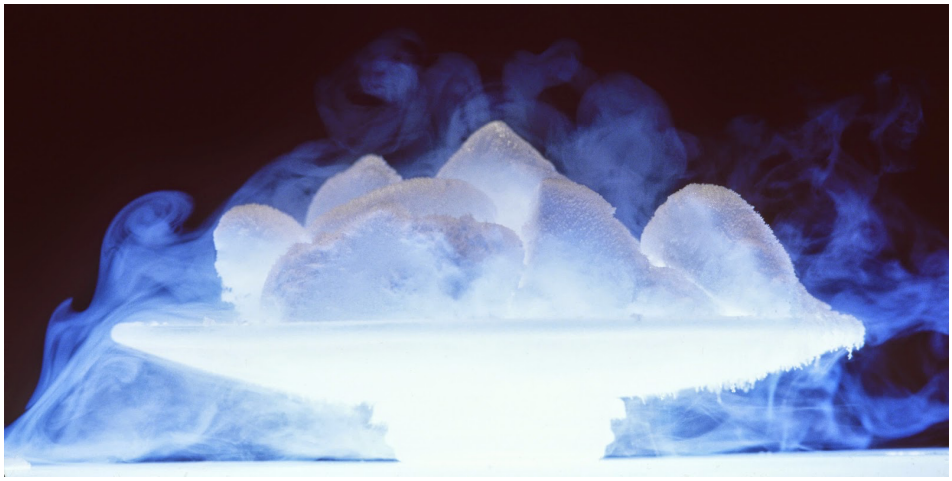

Fig 2.5 – The image of dry ice forming frost on the resting container while sublimating rapidly (the white smoke around the dry ice is the sublimating CO_2 gas).

CHAPTER 3

EXPERIMENTAL DETAILS AND METHODOLOGY

In this chapter, the details of experimental set-ups, approaches and the equipment used to achieve the objective of the current thesis work are discussed in detail. The chapter is organized as follows. We begin this section with the thermal and physical properties of liquid and surfaces used for the experiment and validation for a clear understanding about the materials used in this experiment. It is then followed by the experimental method, objective parameters studied, droplet measurement methods and Image Analysis methods for a more deeper understating of the processes involved in this work to obtain the final goal.

3.1 Materials

3.1.1 Liquid and Surface

The liquid used in the test is n-Hexadecane, 99% (CAS: 544-76-3), purchased from Alfa Aesar Ltd, England. The pure form of n-hexadecane finds application as Phase Change Materials (PCM) in heat and cold storage, commonly known as thermal management systems. Some of the common applications are thermal management in buildings as PCM walls and ceilings that absorb heat, thermoregulating textiles and anti-icing. Hexadecane is chosen as the test fluid because of its low melting point and low latent heat of fusion. This enables us to observe the bounce and splash regime of the fluid at comparatively lower Weber numbers as compared to traditional fluids such as water which have a lower melting point.

The properties of hexadecane such as low melting point and low latent heat causes the droplet to freeze at the interface when it impacts on the dry ice. This phenomenon has uncovered a completely new regime where there is both bouncing of the droplet as well as freezing. To validate the results and condition of hexadecane, the same experiment was repeated for water droplets impacting on the dry ice substrate. The validation was performed to ensure correctness in the results obtained.

The droplet impingement test was conducted on dry ice substrate. The surface of the dry ice was smoothened uniformly by placing a metal plate and applying gentle pressure over it. The main reason behind dry ice being chosen as a target substrate here is that, it has Oleophobic properties which repel most of the organic and inorganic oils. Moreover, the sublimating gas layer on the dry ice acts as a thermal insulation enabling the drops to rebound, glide and hover over the substrate for drops impinging at lower Weber numbers.

Table 3.1: Thermal and Physical Properties of n-Hexadecane and water.

Liquid	**Dynamic Viscosity (μ) mPa**	**Surface Tension (σ) mN/m**	**Density (ρ) Kg/m³**	**Freezing Point °C**	**Weber Number** $We = \frac{\rho v_o^2 D_o}{\sigma}$	**Ohnesorge Number** $Oh = \frac{\mu}{\sigma \rho D_o}$
n-Hexadecane	4.0015 (25°C)	27.47 (20°C)	773	18	13 to 168	0.018
Water	1	72	997	0	13 to 100	0.051

Table 3.2: Properties of Dry ice.

Phase	Temperature °C	Latent Heat of vaporization kj/kg	Specific Gravity Water = 1	Specific Heat kj/kg°C	Density kg/ m^3	Pressure kPa
Gas	-	-	1.539	0.85	1.9769	-
Liquid	-	-	1.18	-	-	-
Solid	-56.6	-	-		-	517.3
	-78.5	-	-	571.3	-	101.3

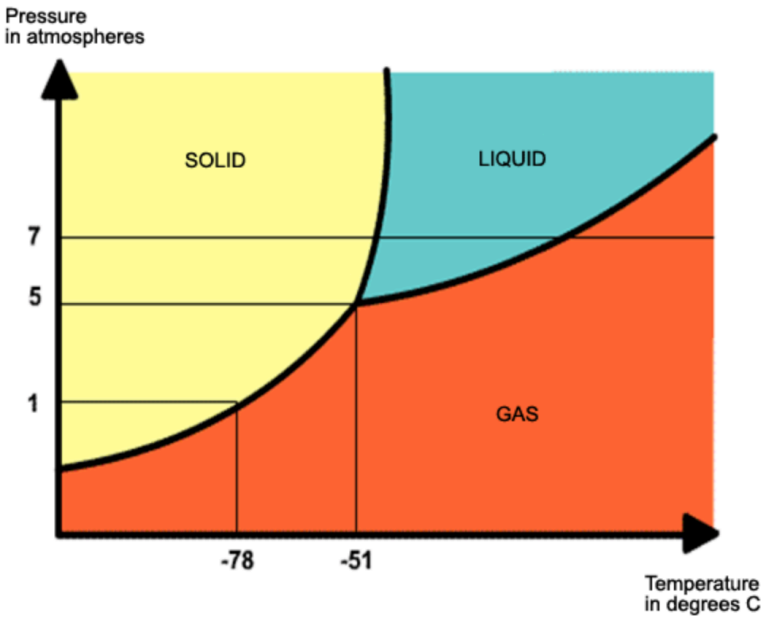

Fig 3.1 – Pressure Vs Temeprature Phase Graph of Carbon dioxide.

3.2 Apparatus

It is desired to study the impingement of the droplet from both side and the top view for a better understanding on the effect of Weber number on drop bouncing and sticking. There is a petal formation regime which can only be studied accurately upon imaging the drop impact from the top view.

3.2.1 Visualization: High Speed Camera Specifications and Orientation

The experimental apparatus for both the side view and top view imaging are the same. However, the imaging techniques differ in the two cases which will be discussed. The experimental setup consists of the following components (a) High-Speed Imaging Unit, (b) Light Unit, (c) Syringe Unit and (d) Processor. The High-Speed Imaging unit is comprised of InfiniProbe^{TM} TS-160 Universal Micro/Macro Imaging Lens mounted onto the Photron FASTCAM Mini AX100 to record slow motion videos. The camera unit was mounted over a lab jack to adjust the height in the Y axis. The Lighting Unit is comprised of a single Nila Zaila light with adjustable intensity mounted over a lab jack. The syringe unit consists of a BD-60ml syringe fitted with a BD PrecisionGlide needle (0.9mm dia * 40mm length). The syringe was mounted vertically over an adjustable stand such that it can be adjusted in the Y axis to obtain different Weber numbers. The processor unit consists of a computer loaded with the Photon (PFV 64bit) software to visualize, capture and process the videos. Dry ice was placed under the needle directly. Uniform lighting was obtained by placing a diffuser plate between the light source and the dry ice. Lighting was adjusted in the X and Y axes to obtain the best lighting condition for high speed imaging.

A scale is very necessary for measuring and analyzing the recorded data. A reticle was used as a scale in this case. The reticle was supported on the plane of drop impact and imaged for future scale image references. It should be carefully noted that the drop impact should be carried out on the same plane of the substrate where the reticle was imaged to obtain accurate measurements.

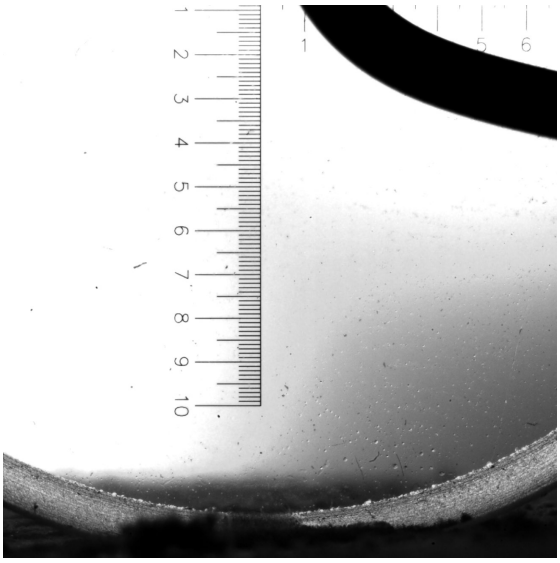

Fig 3.2 - Image of the reticle taken on the plane of droplet impingement

The syringe was filled with n-Hexadecane and fixed on the stand. It should be ensured that it is properly fixed to avoid vibrations. The focus of the camera was set on the right spot by placing an initial droplet on the substrate. Height of the syringe was adjusted, measured and noted using a laboratory scale installed besides the setup. The drop was made to fall on the surface of the dry ice and recorded simultaneously using the PFV software and exported. The same process was repeated for drops impinging from different heights. A series of pictures was recorded during the drop impact with the

following camera settings – 4000fps recording speed and 1024x1024 pixels spatial resolution. Selective frames from the slow-motion capture were selected and exported in a convenient format with a playback speed of 30fps for post-processing.

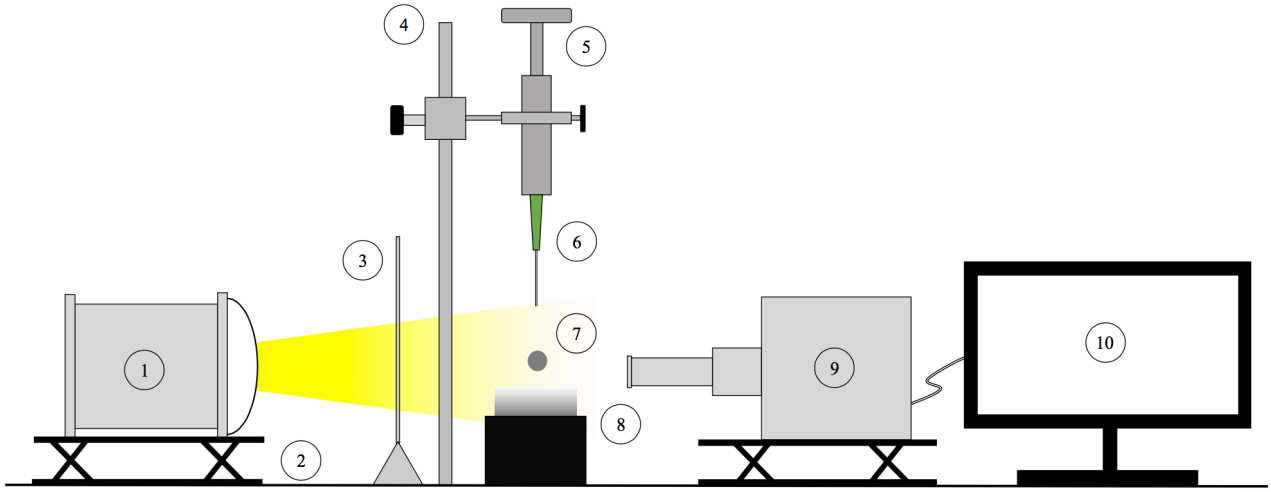

Fig 3.3 - Schematic of the experimental setup for Side View imaging of drop impact. 1 – Light Source, 2 – Lab Jack, 3 – Diffuser Plate, 4 – Stand, 5 – Syringe, 6 – Needle, 7 – Drop, 8 – Dry ice, 9 – High Speed Camera, 10 – Computer

The experimental setup for the top view imaging is the same as that of front view imaging. However, the camera orientation and placement setting was altered to capture the impinging drop from a good top angle to analyze the drop splashing and petal formation. The camera must be mounted in a way that enables easy visualization of drop impact and petal formation. For this purpose, the high-speed camera was set at an angle of approximately 80^0 with respect to the original position of the camera mounted on the tripod stand. Parallax errors and its corrections are not considered because the top view imaging was performed mainly for studying the physical quantities like counting of number of petals for drops impacting from higher Weber numbers.

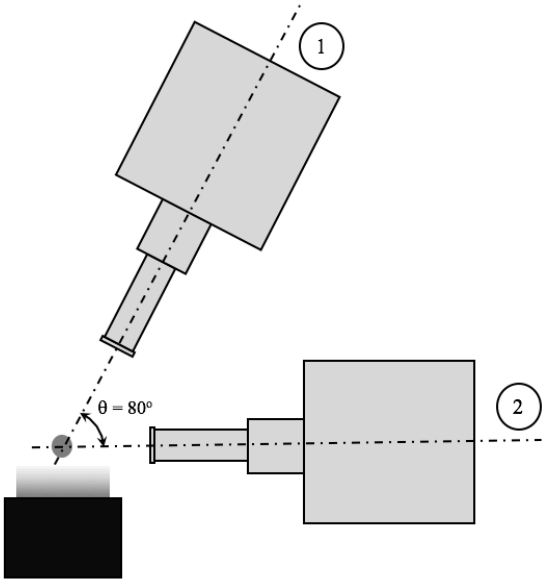

Fig 3.4 - High Speed Camera positions for the two views (top and front) of the drop impact process.
1 – High Speed Camera position for Top View 2 – High Speed Camera position for Front View

3.3 Parameters Studied

There are several parameters that were studied in this experiment which were significant in obtaining critical relationships and trends. The parameters must be comparable with the previously available literatures to make legitimate comparisons, strong theories and proofs. A vast literature study was performed in this topic to obtain the right parameters and relationships that sails the work to its set goals.

3.3.1 List of Parameters and its Significance

Now we will be discussing the various parameters studied in this work along with its significance.

1. **Maximum Spreading Factor of Droplet (D_{max}/D_o):** The maximum diameter of the droplet is required to study and understand the extent to which a droplet spreads upon impact for different Weber numbers.
2. **Spreading Factor of the Droplet w.r.t Time ($D(t)/D_o$):** The spreading factor of the droplet for a given We gives us some information like the speed at which the drop spreads and retracts with time frame. This data helps us calculate the spreading velocity of the droplet.
3. **Number of Petals (N_p):** At lower Weber numbers, non-contactless bouncing of droplet takes place upon impact due to the presence of sublimating layer of dry ice. However, at higher velocities, the droplet breaks the sublimating barrier and impacts on the surface of the substrate directly causing some large changes in diameter (splash regime). During this process, petal like structures are observed. The number of petals is characterized as a function of Weber number.
4. **Contact Time:** The contact time of the droplet is again a function of Weber number. It is defined as the total time in which the droplet is in contact with the substrate before it bounces. This parameter is measurable only for the rebound regime at lower Weber numbers. At the higher Weber numbers, the droplet tends to stick to the substrate upon impact.
5. **Rebound/ Splash Regime Map:** A regime map is an easy representation of the Maximum spreading factor with respect to Weber numbers. This will give a clear understanding of the different regimes that are observed at different Weber numbers

3.4 Measurements connected with Drop Impact

Certain measurements of the impacting drop are necessary to study which will give us the details to ascertain similar initial conditions for all the cases. Similarly, theoretically estimated values like the initial velocity must comply with experimentally determined values to ensure accuracy and the absence of discrepancies in the methodologies followed to obtain the results. For this, the images captured were post-processed and the data-sets were analyzed to obtain the results. The entire drop impact process takes place within 400 frames and selective frames were studied for different parameters.

3.4.1 Sphericity of the Droplet:

The size of the droplet falling from the syringe needle tip - diameter, d was measured from the captured images by post-processing in imageJ software. The hypodermic needle dispensing the droplets demonstrated negligible changes in the shape, which means there was negligible oscillation in the shapes. This was verified by studying the shape factor of the droplet just before the impacting with the substrate. The spherical shape of the droplet was expressed by the following relation,

$$\text{Sphericity} = \frac{6V}{DA}$$

V is the volume of the droplet given by pd3/6 and A is the surface area given by πd^2 where, d is the minimum diameter of the droplet. D is the change in diameter of the droplet with same volume along the perpendicular axis. When D = d, the sphericity of the drop is 1.

The parameters necessary for the measurement of sphericity were measured by *circle fitting* technique in imageJ software. The points of the circle fitting tool were

adjusted such that, it completely captured the shape of the droplet to give accurate measurements in orthogonal directions as show in the Fig. Using the measurements obtained, the sphericity of the droplet was calculated and examined for different Weber numbers. It is clear from the plot that the impacting drop is almost spherical in all the Weber number cases. The sphericity of the droplet can also be calculated by the following formula,

Sphericity $= \frac{Dy}{Dx}$, where $D_y < D_x$.

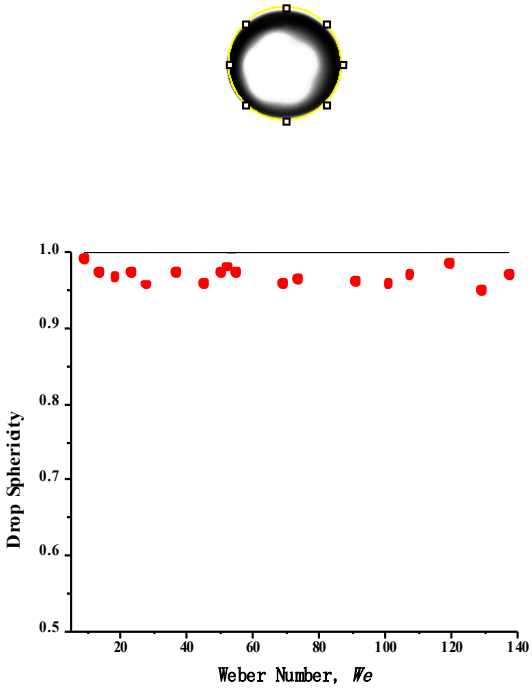

Fig 3.6 – Sphericity of the droplet just prior to the initiation of impact process for different Weber numbers.

3.4.2 Impact Velocity

The impact velocity, Uo of the drop was measured by tracking the falling droplet captured in the high-speed camera. Initial 30 to 60 frames of the high-speed imaging were

used to calculate the impact velocity of the drop. The experimental velocity of the falling water drop before impact is compared with the theoretically estimated velocity of the falling droplet at different heights. Theoretical impact velocity is estimated by the following formula,

$$U_o = \sqrt{2gH}$$

Where, g is the acceleration due to gravity (9.81 m/sec2) and H is the height from which the droplet is released. From the plot, it is evident that the experimentally obtained impact velocity is in good agreement with the theoretical values of U_o. For calculating the impact velocity, the required critical parameters and measurements were obtained by tracing the centroid of the drop using the boundary tracing/ trajectory tool and calculating the difference between the two consecutive points.

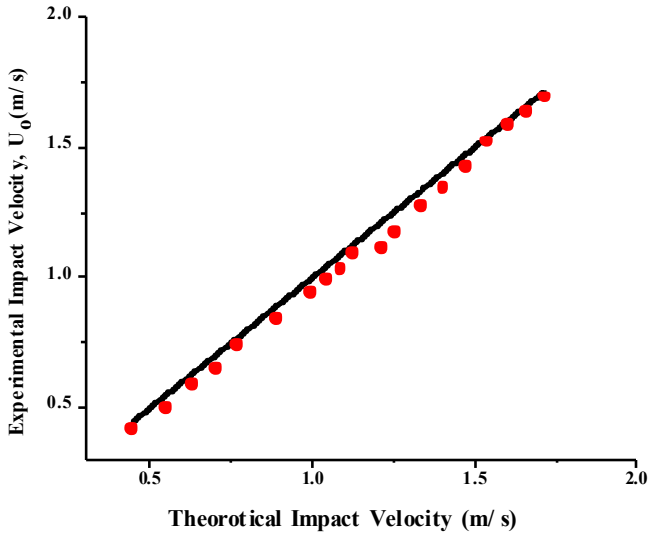

Fig 3.7 – Comparison of experimentally obtained to theoretically obtained impact velocity.

3.5 IMAGE Analysis

In this section, we will be discussing about the steps involved in the processing and analysis of the droplet impact image sequences to obtain the required results. The videos obtained from the high-speed camera are considered as raw image sequences. To analyze these raw sequences, image pre/ post-processing is very necessary. For the image analysis and image processing, two software namely *imageJ* and *Adobe Premier* were used. For generating graphs and plots, *Origin Pro* was used. For image analysis, the following steps were involved in the process – Pre-processing, Solving and Post-processing.

3.5.1 Pre-Processing

This is the first and primary most step in the image analysis. The raw image sequence was imported in the imageJ software and converted to grayscale. Gray scaling is done to reduce the color related noises present in the picture and make the image monotonic in appearance. The scale obtained from the reticle was set initially and them assigned globally for the rest of the analysis. This will ensure uniform measurement system throughout the analysis process. The droplet parameters that need to be measured were checked in the "Set Measurement" option in the Analyze menu. In this process, only the required parameters can be checked while those not required can be neglected to reduce the solving time. The analysis process required high contrast, threshold images with very low to no noises in the work space. The contrast is increased and threshold images are created such that the droplet and the background are in high contrast. Any open holes inside the droplet are filled using the "Fill Hole" tool in the Process menu tab. The region of droplet fall and impact were cropped and maintained to keep the processing and solving time low.

Once the high contrast, threshold image is obtained, the noises and pixel specks in the image needs to be cleared. Options like Despeckle, clear background and Reduce noise in the Noise option can be used. It must be ensured that there are no visible spots, specks or noises in the image to obtain a good output.

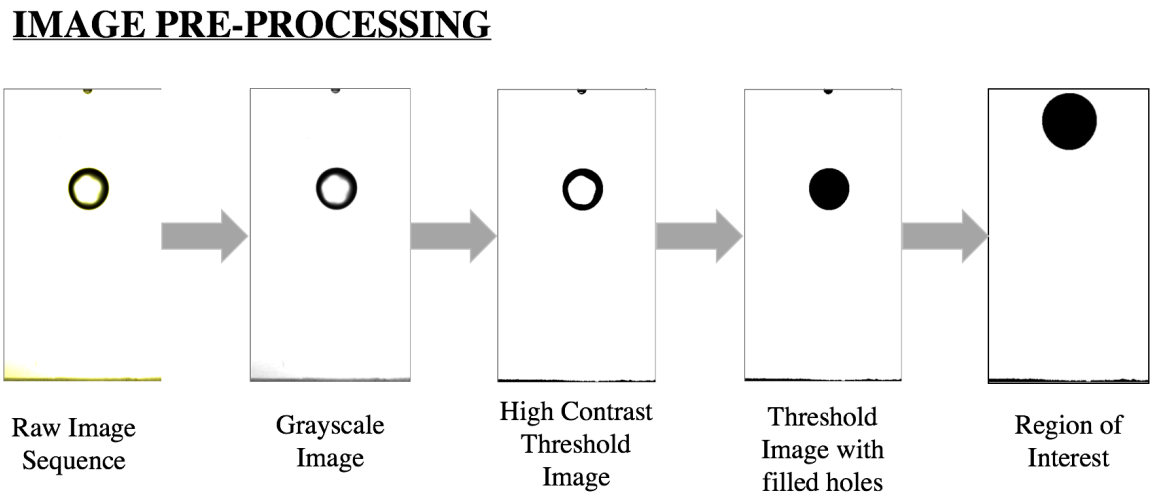

Fig 3.8 – Image pre-processing sequence.

3.5.2 Solving

After pre-processing and preparing the raw data, it is followed by a process called Solving. In this process, all the required parameters for each frame-step is calculated. The solving process is done by the internal algorithm of the software when the specific analysis process is triggered. All the calculation are performed based on the Bounding Rectangle algorithm.

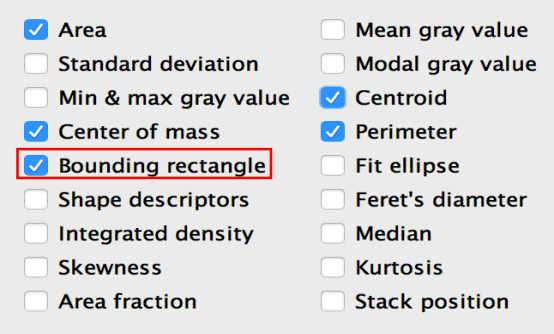

Fig 3.9 – List of parameters selected for measurement in the droplet.

3.5.3 Post-Processing

Post-processing is analyzing the results graphically or by numbers. In this step, the solved results are posted on the screen in the form of decks with all the calculated values of given parameters. Also, the trajectory paths and other visual effects of the drop impact are reconstructed and displayed on the screen to get a clear view about all the parameters computed by the solver. The results obtained include the summary of all the computed parameters, the Region of Interest (ROI) and the time stamp summary which were used for calculation of further parameters related to the droplet.

IMAGE POST-PROCESSING

Results

	Area	XM	YM	Perim.	BX	BY
152	1.211	1.938	3.838	7.889	0.895	3.211
153	1.291	1.929	3.820	7.971	0.926	3.149
154	1.375	1.920	3.807	8.200	0.942	3.102
155	1.453	1.911	3.797	8.319	0.957	3.072
156	1.527	1.905	3.792	8.328	0.988	3.041
157	1.587	1.898	3.785	8.399	1.003	3.010
158	1.638	1.894	3.782	8.557	1.019	2.979
159	2.382E-4	1.752	4.669	0.044	1.744	4.661
160	1.674	1.890	3.783	8.839	1.034	2.964
161	1.699	1.890	3.787	9.155	1.050	2.948

a **b**

Fig 3.9 – Post-processed outputs, a) Result summary of the measured parameters are summarized in the table, b) Trajectories and traced outlines of the droplet impact process at selective frames.

Chapter 4

RESULTS AND DISCUSSION

This Chapter summarizes the experimental observations of n-Hexadecane and Water droplet impact on a supercooled, sublimating substrate. The high-speed images captured were used to make the quantitative assessments of various parameters in the process of droplet impact on the dry ice substrate.

4.1 High Speed Visualization of Droplet Morphologies during the impact on Dry Ice

4.1.1 Impact of Water Droplet

When the droplet impacts on a surface of any nature, it tends to spread on both the sides symmetrically, followed by the receding of the rim inwards, towards the center. Based on the impact velocity, the droplet rebounds or sticks to the surface. Water was used as the baseline test fluid to compare the trends of Hexadecane (actual test liquid) Figure 4.1 illustrates the impact regime of Water droplets for 5 Weber numbers at different time frames depicting different drop dynamics.

The first image in the sequences show the falling water droplet just before collision with the substrate while the remaining images depict the droplet dynamics upon impact at various time frames. The important physics involved in the collision are droplet spreading and the droplet retraction. It can be observed that the rate of spreading increases with increase in Weber number in time frame 3.75ms. At lower and intermediate Weber number ranges (*We = 5.7, 16.7 and 58.73),* droplet rebound is very prominent and can be observed in time frame *t=18.5ms*. No droplet freezing is observed upon contact

or rebound. The drop upon rebound - wobbles in the air continuously and the curvature is maintained at the belly (bottom) of the drop indicating the absence of any freezing front or nucleation upon impact.

However, at higher Weber numbers ($We > 87$) droplet breaking upon impact is observed. At *t=7.5ms,* finger/ petal formation can be observed due to the various instabilities acting at the rim of the spreading droplet. At *t=18.5ms*, droplet breaking or rejection of satellite droplets are observed due to the instabilities overcoming the surface tension of the liquid and conversion of Kinetic Energy into Surface Energy.

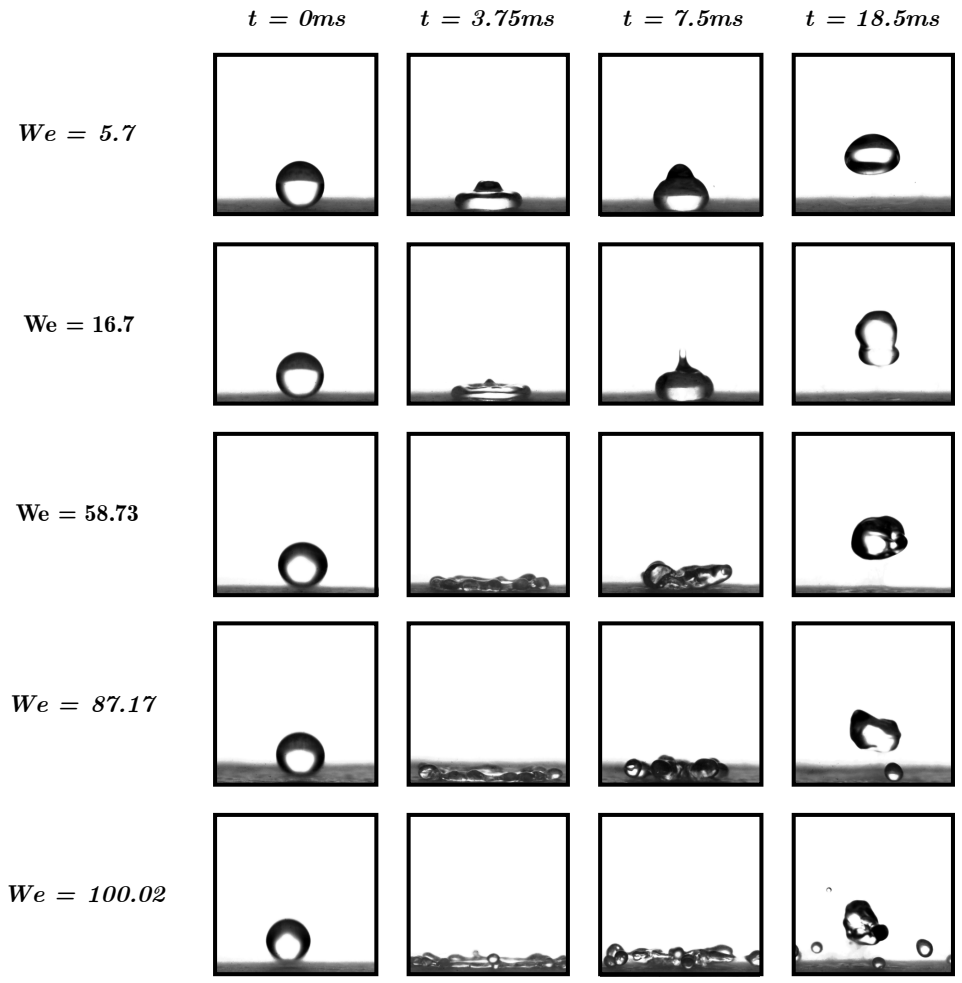

Fig 4.1 – High speed image sequence illustrating the impact of Water droplet of diameter, D_o = 2.4 mm falling from Weber Numbers 5.7, 16.7, 58.73, 87.17 and 100.02 respectively

for the common time frames 0, 3.75, 7.5 and 18.5 ms on the supercooled, sublimating dry ice substrate (in the liquid rebound regime and the freeze + splash regime).

4.1.2 Impact of Hexadecane Droplet

When the droplet impacts on a surface of any nature, it tends to spread on both the sides symmetrically, followed by the receding of the rim inwards, towards the center. Based on the impact velocity, the droplet rebounds or sticks to the surface. Figure 4.2 illustrates the collision of Hexadecane droplets for 5 Weber numbers at different time frames depicting different drop dynamics.

Like the previous case (Water), the first image in the sequence depicts the position of Hexadecane droplet just before collision with the substrate. However, what happens after the impact occurs, differs with that of water. The regimes observed during the Hexadecane droplet impact process on the sublimating substrate is different from that of water due to the physical properties of the liquid itself. For lower Weber numbers ($We = 8.95$ *and 22.36),* the impact process is followed by a very prominent rebound. Here, it is observed that the rebounding droplet does not have a spherical geometry. Instead, there is a flattened belly region in the rebounding droplet which shows the presence and propagation of freezing front (refer time frame $t=18.5ms$).

At higher Weber numbers ($We>80$), the regime observed for Hexadecane is sticking and fragmentation. At higher heights, there is a corresponding increase in velocity. The causes thinning of the droplet during the spreading phase causing faster heat transfer at the thinned, central region. The frozen region arrests the radial movement and inertia of the spreading drop. The effects of instabilities cause the formation of petals/ fingers. Since much of mass is frozen at the lower surface of the drop, the petal retraction is constrained

leading to closure of the fingers like that of a bird claw. Also, no rebound is observed in this case as the inertia is totally arrested and pinned down by freezing. Apart from these, an intermediate regime where petal formation followed by a rebound can be observed within a very small range of Weber number. In Figure 4.2, for *We = 53.62 at t=7.5ms*, petal formation is observed and at *t=18.5ms*, it is followed by a very small rebound. This is because of the conservation of kinetic energy during the collision that resists the droplet from sticking completely upon impact.

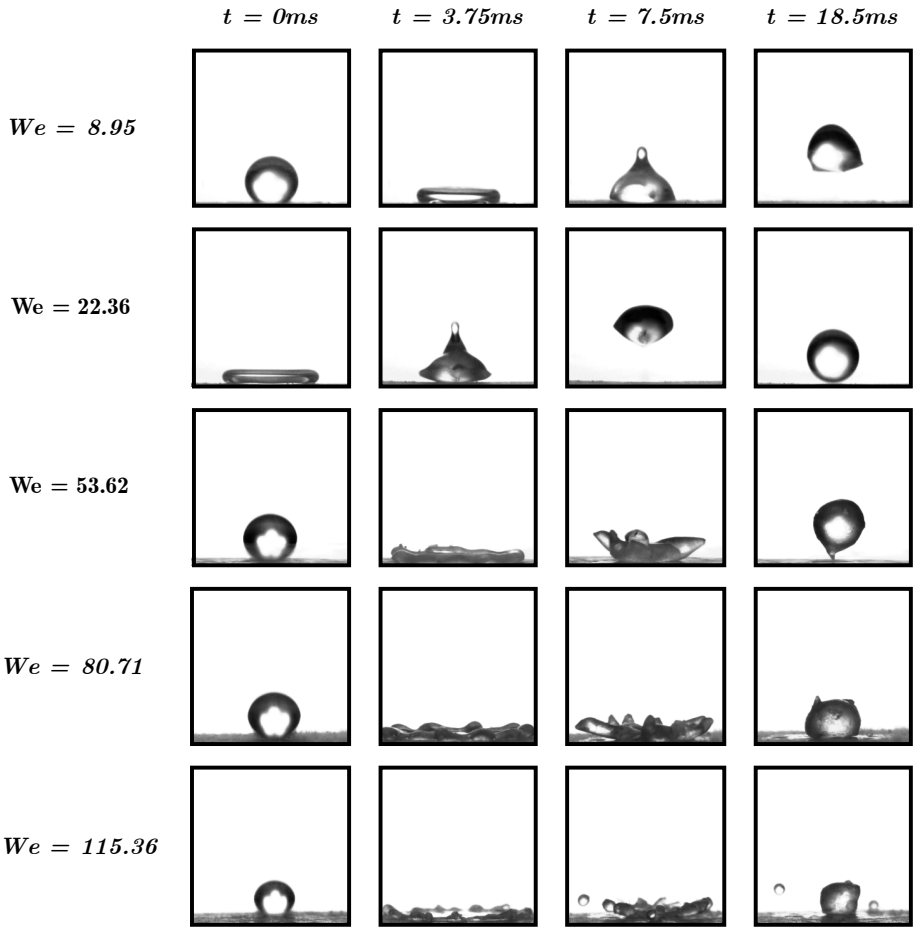

Fig 4.2 – High speed image sequence illustrating the impact of Water droplet of diameter, D_o = 1.667 mm falling from Weber Numbers 8.95, 22.36, 53.62, 80.71 and 115.36 respectively for the common time frames 0, 3.75, 7.5 and 18.5 ms on the supercooled,

sublimating dry ice substrate (in the liquid rebound regime and the freeze + splash regime).

To sum up, the commonly observed morphologies during the hexadecane droplet impact on the supercooled, dry ice substrate are –

a) Spreading Dynamics – When a droplet impacts, it tends to spread symmetrically over its center of impact. The spread os proportional to the impact velocity of the droplet. At higher impacts, the hexadecane drops underwent sticking due to thinning of lamella while water drops broke into fragments and continued to jump.
b) Retracting Dynamics – It is purely based on the kinetic energy and momentum left in the lamella after it has completely spread. For water, the retracting rate is high while for hexadecane it is low. It corresponds inversely to the surface tension of the liquid.
c) Droplet Contactless Rebound – When the water droplet at low to moderate velocities impact on the substrate, the sublimating vapor gas cushions the droplet and helps in rebound.
d) Droplet Contactless Rebound (with partial freezing) – In case of Hexadecane, partial freezing was observed despite the vapor gas layer present which acts as a thermal insulator.
e) Finger Formation + Rebound – When there is improper sticking accompanied by large spreading, this can be observed. (We = 50 to 70 in Hexadecane)
f) Finger formation – Caused due to the K-T instability and high impact velocities of the falling droplet leading to sticking.

g) Finger fragmentation – It is mainly related to the very high impact velocities, leading to thinning of fingers and breakage of the tips into sister droplets due to capillary instabilities.

4.2 Droplet Spreading with Time (D(t) V/s t)

From the literature, the drop impact process is a function of various parameters including that of the liquid, substrate and ambient gas. The spreading of droplet with time is directly dependent on the free-falling droplet impact velocity and its surface tension. The higher the surface tension, the lesser it tends to spread. When there is low surface tension, drop tends to spread more. In our case, the surface tension of hexadecane is lower than water. This causes the drop to spread, leading to thinning of lamella. When the lamella is thin enough, ice nucleation is rapid causing freezing and sticking of the area. To validate this, droplet impact for similar Weber numbers were carried out for Water, but no sticking was observed. This is so because, the high surface tension of Water is ensuring less spread and high contact angle during the impact. Figure 4.3 illustrates the changing droplet diameter peaks with respect to time for 3 different Weber numbers for Water and Figure 4.4 illustrates the changing droplet diameter peaks with respect to time for 5 different Weber numbers for Hexadecane. From Figure 4.3 the diameter of the Water droplet keeps scaling up with higher Weber numbers followed by bouncing, fragmentation or both. Keeping this as a foundation, Hexadecane results are compared for a better insight at changes in the behavior and regimes. From Figure 4.4, it is very clear that for lower Weber numbers (We = *8.997 to 50.36)* of Hexadecane droplet impact, there is a primary peak followed by a secondary peak resembling to that of Water droplet impact

results. This implements that there is a secondary bounce taking place due to the conservation of momentum and energy during the first bounce. The vapor cushion of sublimating gas acts as a thermal barrier and its incompressibility upon drop impingement makes it act as a spring, hence resulting in a rebound.

Now, if we consider higher Weber number ($We>70$), it is observed that the peak is much higher than that of lower Weber numbers. It is obvious because, impact velocity affects the spreading of droplet. The maximum diameter is larger in higher Weber numbers due to the increasing velocity. This high velocity also results in penetration of the droplet into the sublimating gas layer leading to fingerings caused by instability, which will be discussed in the upcoming sub-chapter. Since the drop has penetrated the gas layer, it is in direct contact with the supercooled substrate. Higher velocity also results in large spreading of droplets leading to thinning of the lamella. When the lamella is sufficiently thin, the freezing becomes rapid leading to sticking of the drop to the substrate by means of ice crystal adhesion [27].

There is another case here where the droplet penetrates the sublimating gas layer, but manages to rebound. This can be explained in terms of the thickness of the lamella formed. When the lamella is not too thin for freezing to happen rapidly, then there is a good chance of the droplet escaping the sticking regime even after the formation and retraction of fingers.

In comparison, for the same Weber number range for water, there are just two regimes observed – Total rebound and Rebound with fragmentation. This may be attributed to the fact that water has higher surface tension than hexadecane. The melting

point of water being lower and latent heat being higher than hexadecane helps in sustaining instant freezing upon contact.

Non-dimensionalization of comparable parameter is done to keep the comparison set to same scales. Diameter, D is divided by the initial droplet diameter D_o to homogenize the scale. It is done so because small changes in drop diameter due to scale errors will be adjusted. Time, t is non-dimensionalized by diving it t_o.

$$t_o = t\frac{(U_o)}{D_o}$$

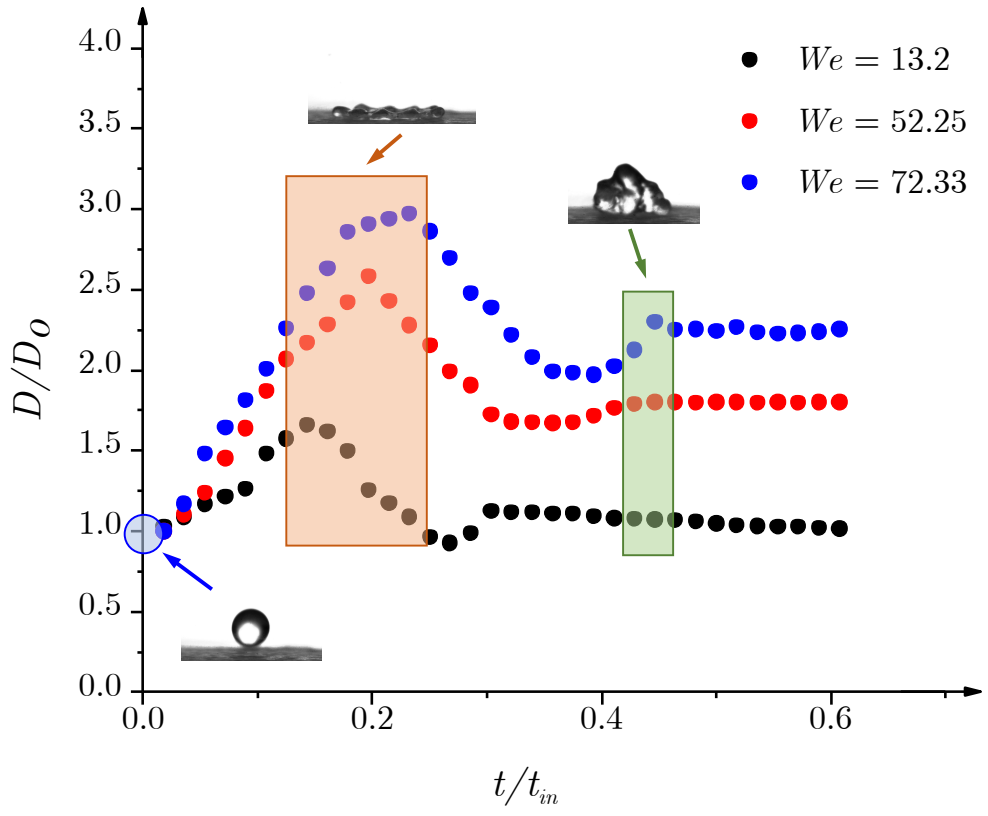

Fig 4.3 – Diameter, D of the droplet spreading with respect to time. D is non-dimensionalized by D_o and time is non-dimensionalized by t_{in}.

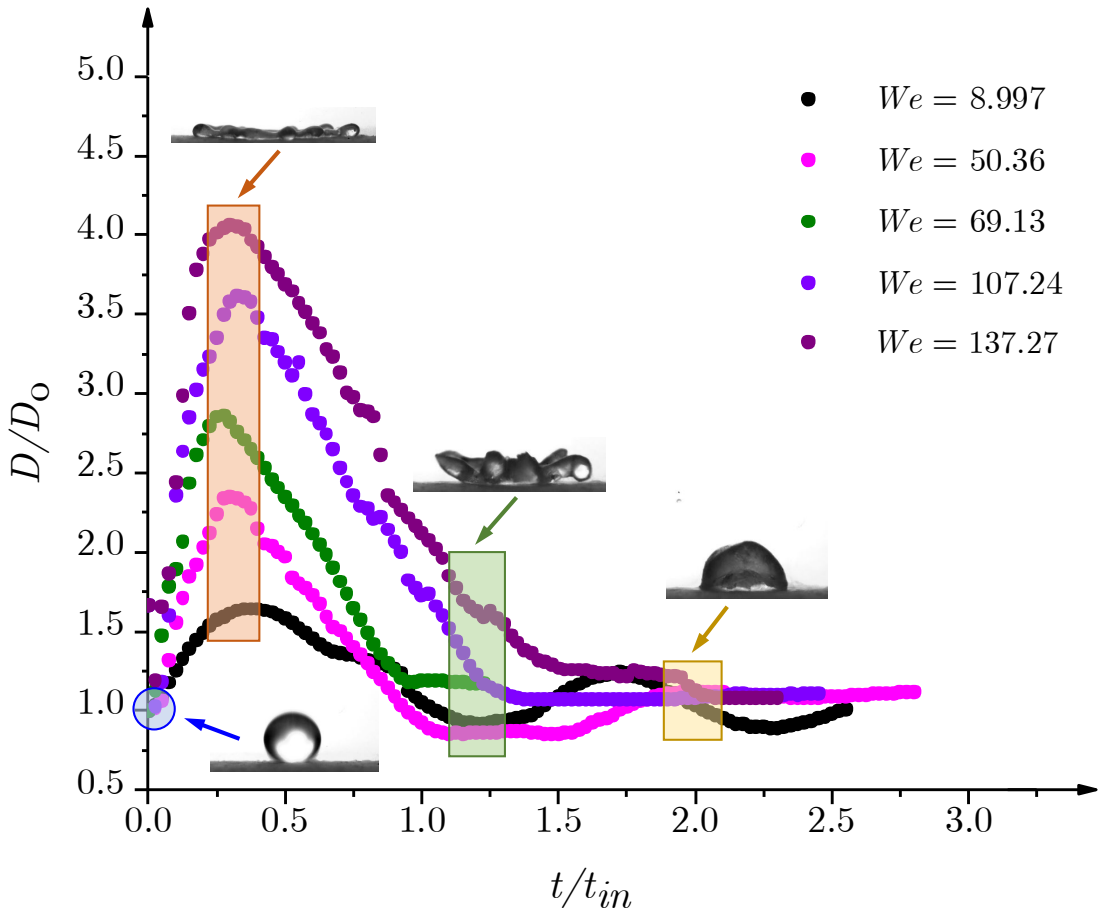

Fig 4.4 – Diameter, D of the droplet spreading with respect to time. D is non-dimensionalized by D_o and time is non-dimensionalized by t_{in}.

4.3 Maximum Spreading Factor – Regime Map

The regime map is usually used to depict different occurrences or phenomena taking place in a single data set. For a given Weber number of a liquid, there can be a unique maximum diameter to which the liquid can spread. The spreading of the liquid is accompanied by multiple occurrences depending upon the regime in which it is in. A completely new regime was uncovered for Hexadecane where partial freezing of the drop was observed along with rebound. To validate this result, it must be scalable with some

known liquid. A validation test was carried out with water droplet for impact on dry ice to compare the results with the available literature. Figure 4.5 illustrates the regime map for water droplet impacting on dry ice. The result obtained for the maximum spread factor with respect to Weber number matches closely to that in literature [26, 41].

$D_{max}/D_0 \sim We^{0.4}$ **(Literature)**

$D_{max}/D_0 \sim We^{0.43}$ **(Present work)**

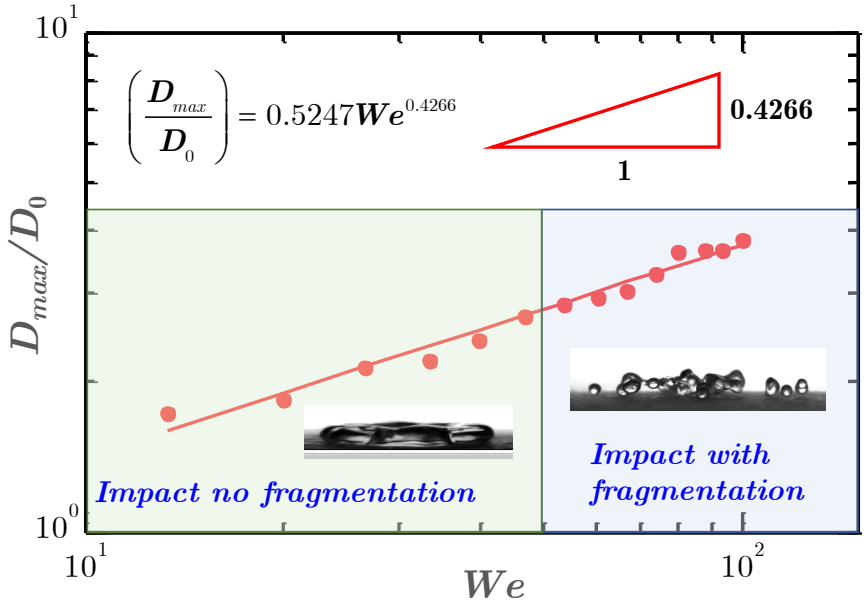

Fig 4.5 – Regime map of water for boiuncing(non-sticking) and fragmentation regime. No sticking is reported until We = 100. Compares to [28]

a) **Bouncing on the sublimating gas** – At low Weber number range i.e. at low impact velocities the water droplet hovers over the layer of sublimating CO_2 gas leading to contactless rebound of the fluid. Figure 4.6 a) illustrates the phenomenon.

b) **Partial Freezing while Bouncing** – The high melting temperature and low latent heat of fusion of the liquid hexadecane causes the drop to lose heat instantly to the

dry ice surface upon proximity. This only reduces the momentum of the droplet resulting a slower rebound compared to water. Figure 4.6 b) illustrates the phenomenon.

c) **Petal/ Finger formation and Bouncing** – Petal formation is mostly attributed to the sticking of the droplet. However, at intermediate Weber number range of 50 - 70, we can clearly observe the formation of fingers accompanied by rebound upon retraction of the fingers. At this point, the drop velocity has helped it make its way through the gas layer over the dry ice but the lack of thinning of lamella has delayed the sticking, leading to some small degree of rebound. Figure 4.6 c) illustrates the phenomenon.

d) **Petal/ Finger formation and complete sticking** – In this regime, the velocity is so high that it facilitates large spreading diameter leading to very thin lamella and thick rims causing it to stick at the center accompanied by petal formation and retraction due to instabilities. Figure 4.6 d) illustrates the phenomenon.

e) **Fragmentation of petals** – This can be observed when the velocity is very high, leading to formation of large fingers. A droplet can hold its shape when in spherical geometry. However, when pulled and thinned, capillary instability causes the tip to break off, leading to sister droplet formation.

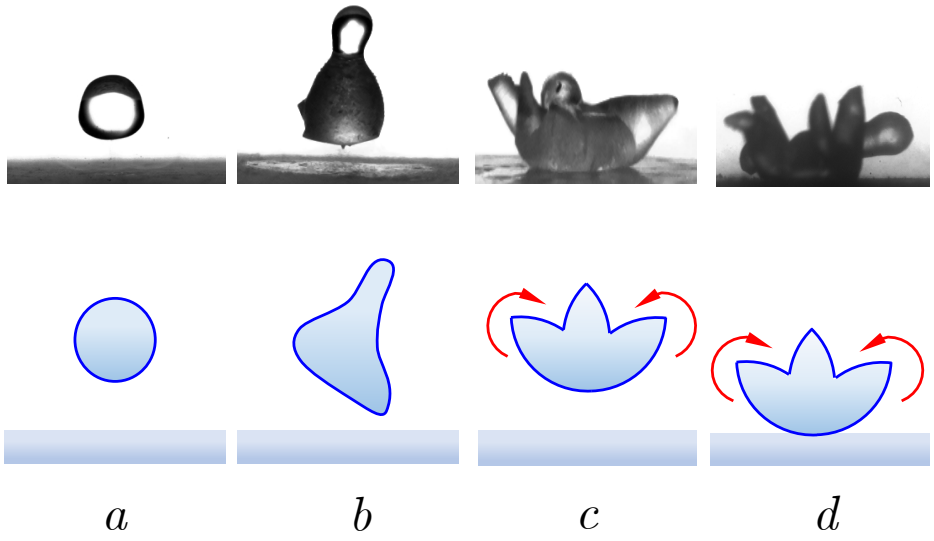

Fig 4.6 – a) Perfect rebound, b) Partial freezing during rebound, c) Petal formation accompanied by rebound and d) Total sticking and petal formation.

Hexadecane was the test fluid to be tested on dry ice. The results obtained was validated by testing water droplet impact on dry ice for similar conditions and comparing it with the literature. Hexadecane droplet of diameter 1.667 mm was generated and impacted on the smoothened dry ice substrate to investigate the effects of impact velocity and Weber number on maximum spreading co-efficient. Hexadecane is a unique fluid which has not been studied much for cold surface impacts. It has high melting point, low surface tension, low heat and low specific heat capacity. These properties of hexadecane have led to the uncovering of certain new findings when impacted on cold surface. Figure 4.6 illustrates the regime map of the Hexadecane. There are three unique regimes observed here –

1. Bouncing + Partial Freezing
2. Fingers + bouncing
3. Total Sticking and Fragmentation

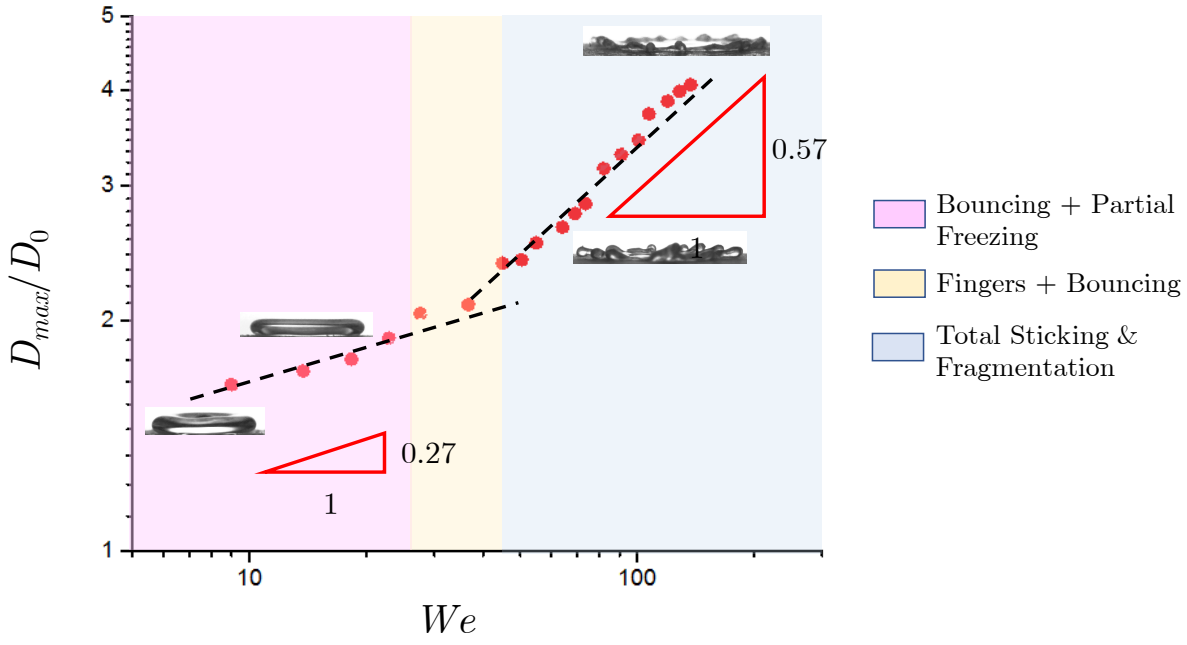

Fig 4.7 – Regime map of the bouncing (non-sticking) + partial freezing regime, Finger formation and bouncing regime; and Total sticking and Fragmentation regime.

For the hexadecane droplet, the relationship between maximum spreading coefficient and Weber number was studied at both bouncing regime as well as sticking regime to compare the results with the previous literature. Also, it is important to check how well does the results on dry ice correlate when compared to tests carried on Super hydrophobic surfaces or Leidenfrost. Figure 4.7 illustrates the maximum spreading factor relation with Weber number for hexadecane at bouncing regime. The freezing at the contact region of the droplet followed by bouncing is resulting in some loss of momentum and kinetic energy after the impact which leads to deviation in the results.

Figure 4.8 illustrates a consolidated comparison of experimental results of Hexadecane and Water on dry ice with the literature and Prof. Paulikakos Universal Relationship.

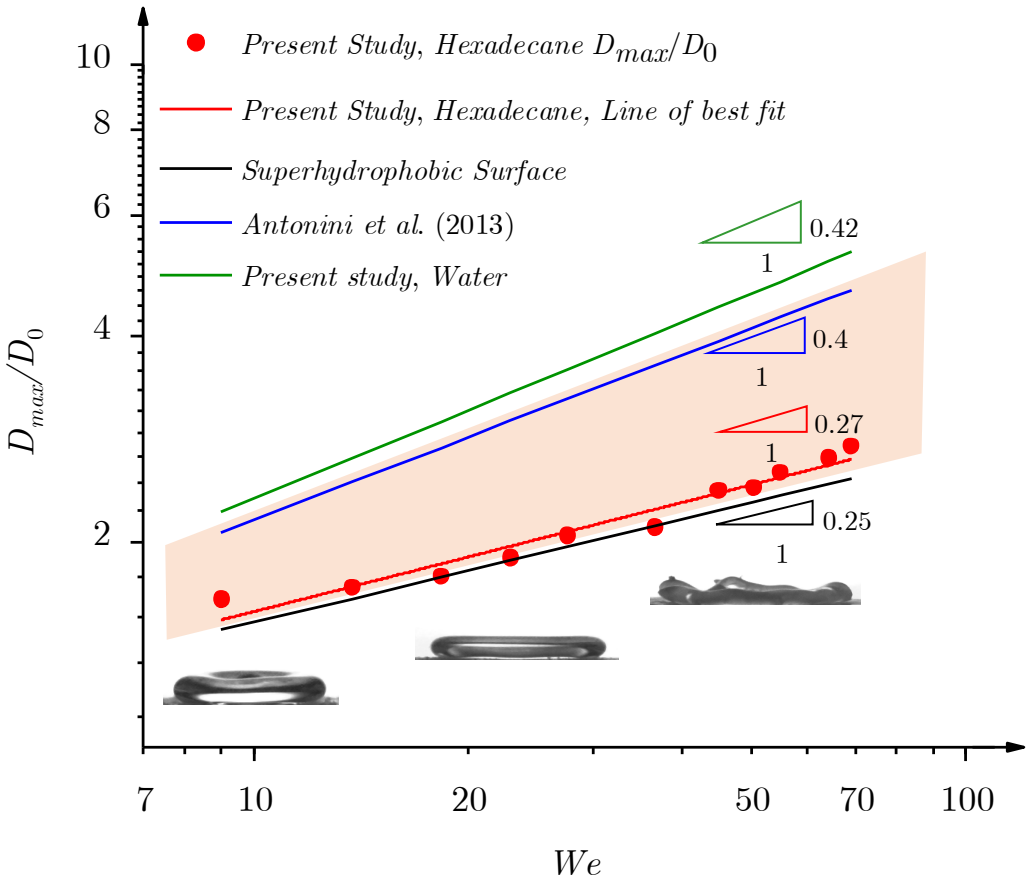

Fig 4.8 – Comparison of the experimental results for hexadecane droplet impact on dry ice for the rebound regime with the results obtained on Super hydrophobic surfaces and Paulikakos Universal relationship [26].

4.4 Contact time (Rebound time)

The contact time of a droplet is the point when the drop touches the substrate to the instant it departs from the surface upon rebound. Basically, the contact time is low for droplets falling at low velocities or low Weber numbers [62]. This is because, the droplet does not spread much while, the surface tension tries to balance the geometry of the drop. When the surface tension is high, sticking happens upon high impact velocities. Figure 4.9 illustrates the sticking time for Hexadecane and Water droplets for a Weber number range of 6 to 60. The contact time of the droplet falls rapidly for weber number

ranges of 1 to 4 and then it appears to be a constant [29, 63]. However, no experimental studies for contact time at high weber number is investigated experimentally. It has been reported in [64] that the contact time increase can be observed after the constant regime at increasing Weber numbers till sticking regime is achieved.

The time of contact is non-dimensionalized by dividing it with the Rayleigh time which gives a close correlation to the contacting time. From the graph, it is evident that the contact time of hexadecane is larger than that of water drops. Since the melting point of hexadecane is high and the specific heat is low, a small heat transfer between the surface and the drop is sufficient to bring the drop to the freezing point. It can be the main reason behind the partial freezing of hexadecane drops upon freezing. A validation test with water shows that the contact time is considerably lower for water, for almost the same range of Weber numbers.

$$t_{Rayleigh} = \frac{\pi}{\sqrt{2}}\sqrt{\frac{\rho D_o^3}{8\sigma}}$$

where ρ - density of fluid, σ - surface tension of fluid, D_o – Diameter of the liquid droplet.

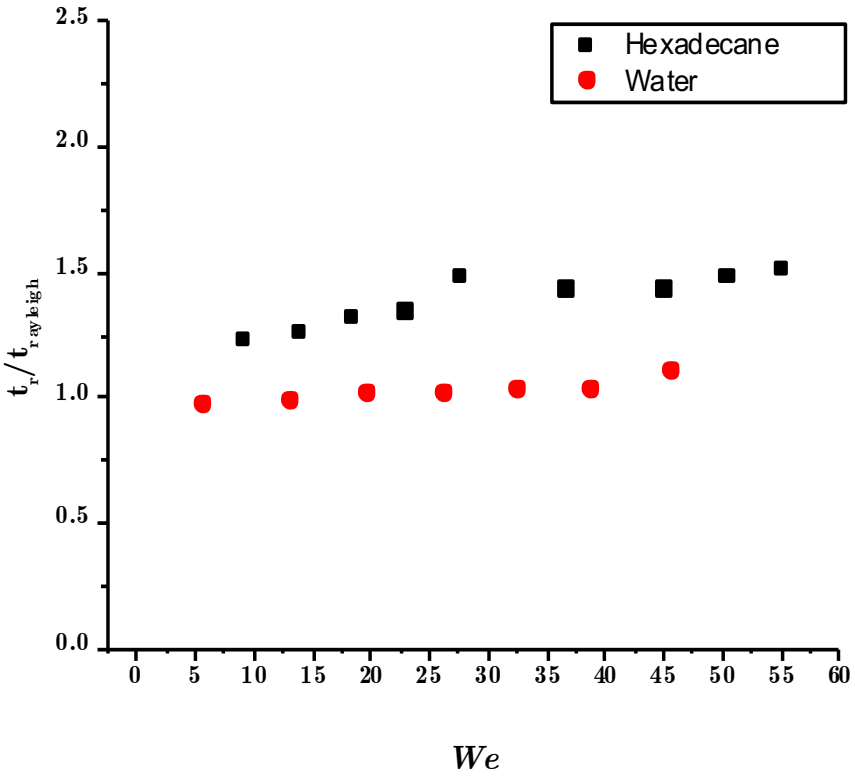

Fig 4.9 – Reationship and comparison of Rebound time with Weber number for water and hexadecane. Rebound time has been non-dimensionalized by Rayleigh time.

4.5 Rebound Velocity

The impact velocity of a free-falling droplet is quite not a controllable parameter. The theoretically computed value correlates closely with the experimental results. However, the rebound velocity is not simple to determine. Based on the sticking nature of the drop and temperature of the substrate, the rebound velocity can change greatly [65-68]. For example, a surface may exhibit super hydrophobicity at room temperature but may cause sticking at low temperatures. This is because of the Casie-Baxter to Wenel State transformation. When the liquid drop parameters such as droplet temperature, surface tension and dynamic viscosity changes, the rebound velocity may be altered. In

our case, we compare the rebound velocity of the hexadecane droplet on dry ice with results obtained for water drops impacting on dry ice. The validation of water drop test on dry ice was compared to literature [64] and found out that the rebound velocity on dry ice is slightly lower than that of SHS. We expect the result for hexadecane to follow similar trends. Figure 4.9 a) shows the result of the ratio of rebound to impact velocity with respect to impact velocity. A good downward trend is observed for the Weber number range which shows the transition of water from the rebound to sticking regime. A point to note here is that, water has high surface tension which delays the sticking process. Hence, very high velocity is required to see the sticking of water droplets on supercooled surfaces. The high surface tension also causes the droplet to break easily in satellite droplets.

When we compare Hexadecane with water, it has a surface tension of order 4 times smaller. This means, Hexadecane can spread more than water causing the sticking regime to be observable at lower Weber number range. Total Bouncing regime in Hexadecane mostly occurs at very low Weber numbers ($We < 10$). So, there is some resistance even though the drop seems to bounce at a range beyond the above-mentioned Weber number. We justify this by the observations made during the experiment where, the droplet began freezing partially right upon impact. So, when it rebounded, a flat, frozen layer of the droplet was observed which is said to damp the recoil velocity of the droplet. The freezing process turns the liquid into a solid mass of higher density and hence arresting momentum. Figure 5.0 shows the result of the ratio of rebound to impact velocity of the Hexadecane droplet on dry ice. It is clearly seen that the rebound velocity is much smaller than that of water at Weber number range of 5 to 8. This Is a clear demonstration of loss of

momentum in the droplet due to frozen mass at the bottom of the droplet. Theories speak that the gas layer mostly acts as insulating barriers. In this case, the specific heat of hexadecane is very low. This can cause rapid fall in temperature by removing very less heat from the drop compared to water. The melting point of hexadecane is high (17° C) which is a few degrees lower than the room temperature. When the droplet is in close vicinity of the substrate, the drop begins to give away large amount of heat causing some supercooling effects. This drop upon impact on the cushion layer can initiate nucleation due to the gradient in pressure inside the drop itself. Hexadecane is one such fluid that falls in the freeze/bunce regime.

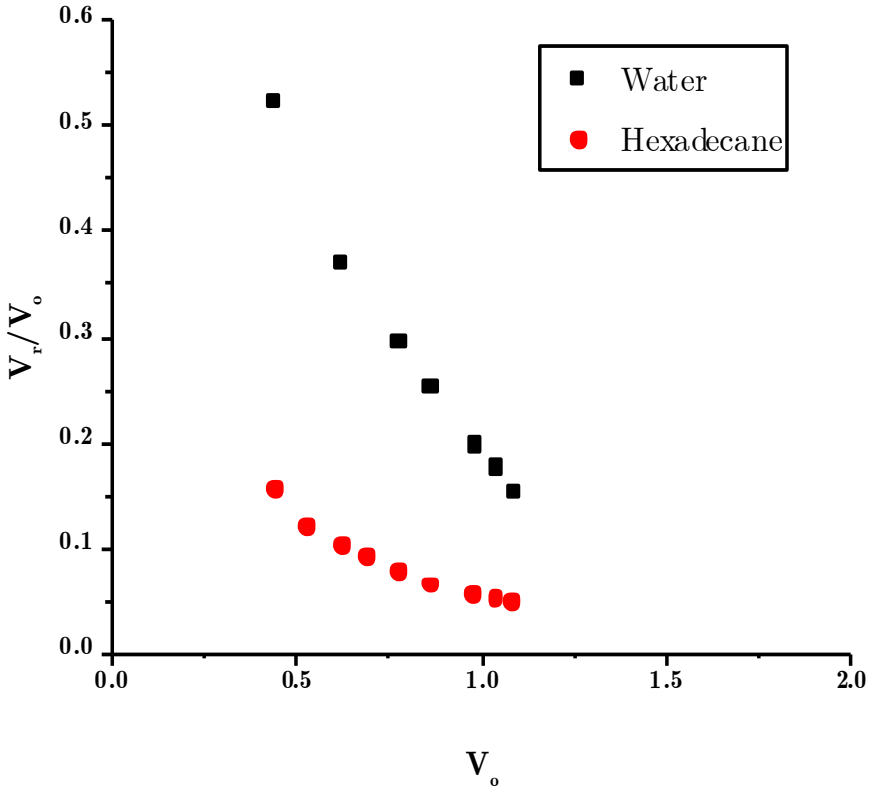

Fig 5.0 – The comparison of rebound of droplet with initial velocity.

4.6 Petal Formation – Regime Map

Petal formation or fingering is a beautiful occurrence that can be observed when there is instability in a system. Rayleigh-Taylor instability is the physics behind the fingering process. Whenever, there is a denser fluid over a fluid of comparatively lesser density, rapid mixing occurs to attain thermodynamic equilibrium. During this mixing process, finger like patterns are observed [69, 70]. In this case, the droplet density is much higher than the sublimating CO_2 gas layer density. Fingering occurs when the droplet falling at high impact velocity enters the layer of CO_2 gas, the rapid mixing movement of gas around the liquid during the spreading process subjects the liquid to form crests on the rim perimeter. These crests develop into full featured petals when the lamella freezes while the rim is still in motion. These finger like structures are balanced by surface tension between the liquid and the gas [71]. Hence, there contract back like a closing claw. One important objective of this work is counting the number of fingers formed for different drop impact heights. By arranging a top view imagine technique as discussed in Chapter 3, we could capture images for quantitative counting purpose. The fingering phenomenon follows a specific trend for different types of surfaces. For dry ice, the results have been interpreted in Figure 5.1. The first regime in the no petal regime or the rebound regime. Petals begin to appear at the splashing regime. However, distinctive petals can be observed at the rebound regime too close to the transition point of sticking regime. The N_f scaling is roughly 0.99 times Weber number in our work. It is lesser than the values proposed by Thoroddsen, which is roughly 1.8 times Weber number on linen papers [58]. This shows that the substrate plays an important role in the petal formation phenomenon.

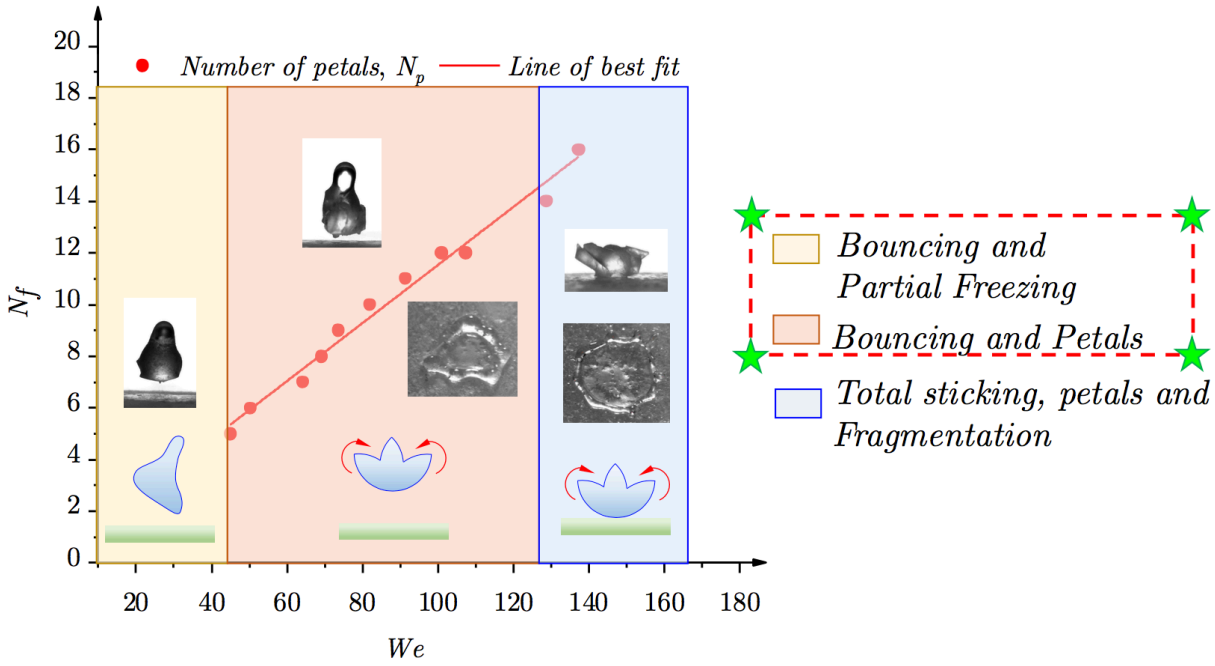

Fig 5.1 – Petal formation regime map for the number of petals formed at different weber numbers for Hexadecane.

Chapter 5

SUMMARY AND CONCLUSION

The ultimate objective of this work is to study the impact process of Hexadecane on dry ice and compare it with the literature and validate with the water impact test conducted on dry ice substrate. Petal formation regime was the focus of the work however, some interesting phenomenon were observed at the droplet rebound regime itself which was not reported in the literatures. In this work, a careful and systematic investigation of hexadecane and water droplets impinging on a sublimating surface was studied to compare its surface characteristics and its behavior.

5.1 Key Findings

This experimental investigation has revealed some very interesting drop impact dynamics which were not reported in the literature. The major conclusions of this work are as follows -

a) Hexadecane droplet impact on a supercooled surface (dry ice) is a non-contact impact process where the fluid drop doesn't meet the substrate directly. This work uncovers a noble, new regime in drop rebound called as "rebound with partial freezing".

b) The partial freezing interface is due to the low surface tension of the fluid that enables it to spread more than liquids with higher surface tension.

c) Hexadecane has high melting point and low specific and latent heat of fusion. This causes sudden drop in temperature of the fluid drop prior and upon impact on the substrate.

d) At the rebound regime, the results for hexadecane for the maximum spreading factor deviates with the Universal maximum spreading diameter relationship proposed by Paulikakos et al. This is because of the of the partial freezing during the spreading that resists the motion of fluid.

e) The maximum spreading factor of water was tested on dry ice to validate the above obtained results. Water followed the trend mentioned by Paulikakos et al.

f) The spreading of Hexadecane drop with time followed a trend which agrees to the literature. An upslope followed by downslope after a peak value was observed. In low velocity cases, secondary peak was observed which was attributed to the droplet rebound. As the Weber number increases, the upslope becomes steeper (indicating faster spreading) and the downslope become shallow (indicating slower rebound velocity).

g) The contact time graph shows that Hexadecane has higher contact time than water upon impact for similar Weber numbers. This answers to the question why the drop is partially frozen during the rebound and why the petals contract like claws.?

h) The rebound velocity of Hexadecane droplet shows damped results compared to water. This is due to the low surface tension of Hexadecane. The drop begins to freeze forming a solid interface, leading to loss of momentum and hence, damping the droplet movement.

i) The splashing regime saw the formation of petals followed by unique retraction of petals that looked like closing claws of a bird. The formation of petals is attributed to the Rayleigh-Taylor instability at the liquid-gas interface. However, the retraction of petals is related to some heat transfer. The lamella formation and thinning mechanics of hexadecane shows that rapid freezing causes sticking of thinned lamella. The bottom layer of the droplet is frozen while the mass above is liquid. The frozen layer affects the dynamics, causing the fingers/ petals to curl upward and retract. The scaling is comparatively different from the Thoroddsen results and Paulikakos work. This clearly states the dependence of surface chemistry and surface property on the fingering phenomenon.

5.2 Future Work

Droplet impact studies and interaction with different surfaces has large applications in laboratories and industries. Though it is a well-established field in Science and Engineering, there are some dark faces yet to be justified or discovered. Once such uncovered finding in this work is the "bouncing with partial freezing" regime and the change in retraction dynamics during splashing of hexadecane drops leading to curling up of the petals. There were several questions encountered during the study of droplet interaction which could not find appropriate answers at this point of time due to time constraints and lack of data acquisition techniques. However, it is healthy to suggest improvements and studies that could optimize the study of droplet interaction with surfaces. Some of the suggestion for the future work, that I feel is worthy are –

a) Study of liquids with high melting points and low specific and latent heat must be studied on dry ice (or other supercooled sublimating surfaces).

b) The thermal mapping of droplets could answer questions related to the thermodynamic balance and heat transfer in the drop during impact.

c) The formation of crater during the impact is attributed to the heat absorbed by the dry ice from the droplet. The study of crater diameter and depth could tell us the amount of heat transfer between the drop and the substrate.

Reference

[1] B. R, "Self-cleaning surfaces - virtual realities," *Nature Materials,* vol. 2, no. 1, pp. 301-306, 2003.

[2] L. Hulse-Smith, N. Z. Mehdizadeh, and S. Chandra, "Deducing drop size and impact velocity from circular bloodstains," *Journal of forensic science,* vol. 50, no. 1, pp. JFS2003224-10, 2005.

[3] W.-K. Hsiao, I. Hutchings, S. Hoath, and G. Martin, "Ink jet printing for direct mask deposition in printed circuit board fabrication," *Journal of Imaging Science and Technology,* vol. 53, no. 5, pp. 50304-1-50304-8, 2009.

[4] L. Meyers and G. W. Frasier, "Creating hydrophobic soil for water harvesting," *Journal of Irrigation and Drainage Engineering,* 1969.

[5] M. Sehmbey, M. Pais, and L. Chow, "Effect of surface material properties and surface characteristics in evaporative spray cooling," *Journal of thermophysics and heat transfer,* vol. 6, pp. 505-512, 1992.

[6] M. Rein, "Phenomena of liquid drop impact on solid and liquid surfaces," *Fluid Dynamics Research,* vol. 12, no. 2, pp. 61-93, 1993.

[7] T. Darmanin and F. Guittard, "Superhydrophobic and superoleophobic properties in nature," *Materials Today,* vol. 18, no. 5, pp. 273-285, 2015.

[8] R. N. Wenzel, "Resistance of solid surfaces to wetting by water," *Industrial & Engineering Chemistry,* vol. 28, no. 8, pp. 988-994, 1936.

[9] A. Cassie and S. Baxter, "Wettability of porous surfaces," *Transactions of the Faraday society,* vol. 40, pp. 546-551, 1944.

[10] S. S. Latthe, A. B. Gurav, C. S. Maruti, and R. S. Vhatkar, "Recent progress in preparation of superhydrophobic surfaces: a review," *Journal of Surface Engineered Materials and Advanced Technology,* vol. 2, no. 02, p. 76, 2012.

[11] J. T. Simpson, S. R. Hunter, and T. Aytug, "Superhydrophobic materials and coatings: a review," *Rep Prog Phys,* vol. 78, no. 8, p. 086501, Jul 2015.

[12] L. Ejenstam, "Hydrophobic and superhydrophobic coatings for corrosion protection of steel," KTH Royal Institute of Technology, 2015.

[13] E. Aljallis, M. A. Sarshar, R. Datla, V. Sikka, A. Jones, and C.-H. Choi, "Experimental study of skin friction drag reduction on superhydrophobic flat plates in high Reynolds number boundary layer flow," *Physics of Fluids,* vol. 25, no. 2, p. 025103, 2013.

[14] J. Zhang, H. Tian, Z. Yao, P. Hao, and N. Jiang, "Mechanisms of drag reduction of superhydrophobic surfaces in a turbulent boundary layer flow," *Experiments in Fluids,* vol. 56, no. 9, p. 179, 2015.

[15] B. J. Basu and V. Dinesh Kumar, "Fabrication of Superhydrophobic Nanocomposite Coatings Using Polytetrafluoroethylene and Silica Nanoparticles," *ISRN Nanotechnology,* vol. 2011, pp. 1-6, 2011.

[16] J. De Ruiter, R. Lagraauw, D. Van Den Ende, and F. Mugele, "Wettability-independent bouncing on flat surfaces mediated by thin air films," *Nature Physics,* Letter vol. 11, no. 1, pp. 48-53, 11/10/online 2015.

[17] L. Duchemin and C. Josserand, "Curvature singularity and film-skating during drop impact," (in English), *Physics of Fluids,* vol. 23, no. 9, 2011, Art. no. 091701.
[18] J. De Ruiter, J. M. Oh, D. Van Den Ende, and F. Mugele, "Dynamics of collapse of air films in drop impact," *Physical Review Letters,* vol. 108, no. 7, // 2012.
[19] V. Kulkarni, D. Guildenbecher, and P. Sojka, "Secondary atomization of newtonian liquids in the bag breakup regime: Comparison of model predictions to experimental data," in *ICLASS 2012, 12th International Conference on Liquid Atomization and Spray Systems, Heidelberg, Germany*, 2012.
[20] V. Kulkarni and P. Sojka, "Bag breakup of low viscosity drops in the presence of a continuous air jet," *Physics of Fluids,* vol. 26, no. 7, p. 072103, 2014.
[21] S. Anand and K. K. Varanasi, "Articles and methods for levitating liquids on surfaces, and devices incorporating the same," ed: Google Patents, 2013.
[22] T. Tran, H. J. Staat, A. Prosperetti, C. Sun, and D. Lohse, "Drop impact on superheated surfaces," *Phys Rev Lett,* vol. 108, no. 3, p. 036101, Jan 20 2012.
[23] J. G. Leidenfrost, "On the fixation of water in diverse fire," *International Journal of Heat and Mass Transfer,* vol. 9, no. 11, pp. 1153-1166, 1966.
[24] B. S. Gottfried, C. J. Lee, and K. J. Bell, "The leidenfrost phenomenon: film boiling of liquid droplets on a flat plate," *International Journal of Heat and Mass Transfer,* vol. 9, no. 11, pp. 1167-1188, 1966.
[25] A. L. Biance, C. Clanet, and D. Quéré, "Leidenfrost drops," *Physics of Fluids,* Article vol. 15, no. 6, pp. 1632-1637, 2003.
[26] J. Moláček and J. W. Bush, "Drops bouncing on a vibrating bath," *Journal of Fluid Mechanics,* vol. 727, pp. 582-611, 2013.
[27] J. Kolinski, "The role of air in droplet impact on a smooth, solid surface," Harvard University, 2015.
[28] Y. Couder, E. Fort, C. H. Gautier, and A. Boudaoud, "From bouncing to floating: noncoalescence of drops on a fluid bath," *Phys Rev Lett,* vol. 94, no. 17, p. 177801, May 06 2005.
[29] C. Antonini, I. Bernagozzi, S. Jung, D. Poulikakos, and M. Marengo, "Water drops dancing on ice: how sublimation leads to drop rebound," *Phys Rev Lett,* vol. 111, no. 1, p. 014501, Jul 05 2013.
[30] K. K. Varanasi, T. Deng, J. D. Smith, M. Hsu, and N. Bhate, "Frost formation and ice adhesion on superhydrophobic surfaces," *Applied Physics Letters,* vol. 97, no. 23, p. 234102, 2010.
[31] W. D. Flower, "The terminal velocity of drops," *Proceedings of the Physical Society,* vol. 40, no. 1, p. 167, 1927.
[32] A. Green, "An approximation for the shapes of large raindrops," *Journal of Applied Meteorology,* vol. 14, no. 8, pp. 1578-1583, 1975.
[33] A. F. Spilhaus, "Drop size, intensity, and radar echo of rain," *Journal of Meteorology,* vol. 5, no. 4, pp. 161-164, 1948.
[34] J. E. McDonald, "The shape of raindrops," *Sci. Am,* vol. 190, no. 2, pp. 64-68, 1954.
[35] J. E. McDonald, "The shape and aerodynamics of large raindrops," *Journal of Meteorology,* vol. 11, no. 6, pp. 478-494, 1954.

[36] E. Lac and J. Sherwood, "Motion of a drop along the centreline of a capillary in a pressure-driven flow," *Journal of Fluid Mechanics,* vol. 640, pp. 27-54, 2009.

[37] B. Z. Vamerzani, M. Norouzi, and B. Firoozabadi, "Analytical solution for creeping motion of a viscoelastic drop falling through a Newtonian fluid," *Korea-Australia Rheology Journal,* vol. 26, no. 1, pp. 91-104, 2014.

[38] T. Young, "An essay on the cohesion of fluids," *Philosophical Transactions of the Royal Society of London,* vol. 95, pp. 65-87, 1805.

[39] D. Bartolo, F. Bouamrirene, É. Verneuil, A. Buguin, P. Silberzan, and S. Moulinet, "Bouncing or sticky droplets: Impalement transitions on superhydrophobic micropatterned surfaces," (in English), *Europhysics Letters,* Article vol. 74, no. 2, pp. 299-305, 2006.

[40] A. L. Yarin, "Drop impact dynamics: Splashing, spreading, receding, bouncing," in *Annual Review of Fluid Mechanics* vol. 38, ed, 2006, pp. 159-192.

[41] M. Remer *et al.*, "Dynamic contact of droplet with superhydrophobic surface in conditions favour icing," in *Journal of Physics: Conference Series*, 2014, vol. 530, no. 1, p. 012028: IOP Publishing.

[42] A. M. Worthington, *A study of splashes*. Longmans, Green, and Company, 1908.

[43] A. Yarin, "Drop impact dynamics: splashing, spreading, receding, bouncing...," *Annu. Rev. Fluid Mech.,* vol. 38, pp. 159-192, 2006.

[44] R. Zhao, Q. Zhang, H. Tjugito, and X. Cheng, "Granular impact cratering by liquid drops: Understanding raindrop imprints through an analogy to asteroid strikes," *Proceedings of the National Academy of Sciences,* vol. 112, no. 2, pp. 342-347, December 29, 2014 2015.

[45] M. A. Nearing, J. M. Bradford, and R. D. Holtz, "Measurement of force vs. time relations for waterdrop impact," (in English), *Soil Science Society of America Journal,* vol. 50, no. 6, pp. 1532-1536, 1986.

[46] C. Antonini, F. Villa, I. Bernagozzi, A. Amirfazli, and M. Marengo, "Drop rebound after impact: the role of the receding contact angle," *Langmuir,* vol. 29, no. 52, pp. 16045-50, Dec 31 2013.

[47] C. Hao *et al.*, "Superhydrophobic-like tunable droplet bouncing on slippery liquid interfaces," *Nat Commun,* vol. 6, p. 7986, Aug 07 2015.

[48] D. Richard, C. Clanet, and D. Quéré, "Surface phenomena: Contact time of a bouncing drop," *Nature,* vol. 417, no. 6891, p. 811, 2002.

[49] J. C. Bird, S. S. H. Tsai, and H. A. Stone, "Inclined to splash: Triggering and inhibiting a splash with tangential velocity," *New Journal of Physics,* vol. 11, // 2009.

[50] R. Rioboo, C. Tropea, and M. Marengo, "Outcomes from a drop impact on solid surfaces," *Atomization and Sprays,* vol. 11, no. 2, pp. 155-165, // 2001.

[51] S. Schiaffino and A. A. Sonin, "Molten droplet deposition and solidification at low Weber numbers," *Physics of Fluids,* vol. 9, no. 11, pp. 3172-3187, // 1997.

[52] E. Villermaux and B. Bossa, "Drop fragmentation on impact," *Journal of Fluid Mechanics,* vol. 668, pp. 412-435, 2011.

[53] V. Grishaev, C. S. Iorio, F. Dubois, and A. Amirfazli, "Complex Drop Impact Morphology," *Langmuir,* vol. 31, no. 36, pp. 9833-44, Sep 15 2015.

[54] J. de Ruiter, R. E. Pepper, and H. A. Stone, "Thickness of the rim of an expanding lamella near the splash threshold," *Physics of Fluids,* vol. 22, no. 2, pp. 1-9, // 2010.

[55] I. V. Roisman, R. Rioboo, and C. Tropea, "Normal impact of a liquid drop on a dry surface: Model for spreading and receding," (in English), *Proceedings of the Royal Society A: Mathematical, Physical and Engineering Sciences,* Article vol. 458, no. 2022, pp. 1411-1430, 2002.

[56] J. Fukai *et al.*, "Wetting effects on the spreading of a liquid droplet colliding with a flat surface: Experiment and modeling," *Physics of Fluids,* vol. 7, no. 2, pp. 236-247, // 1995.

[57] J. Liu, H. Vu, S. S. Yoon, R. A. Jepsen, and G. Aguilar, "Splashing phenomena during liquid droplet impact," *Atomization and Sprays,* vol. 20, no. 4, 2010.

[58] S. T. Thoroddsen and J. Sakakibara, "Evolution of the fingering pattern of an impacting drop," *Physics of Fluids,* vol. 10, no. 6, pp. 1359-1374, 1998.

[59] N. Z. Mehdizadeh, S. Chandra, and J. Mostaghimi, "Formation of fingers around the edges of a drop hitting a metal plate with high velocity," (in English), *Journal of Fluid Mechanics,* Article no. 510, pp. 353-373, 2004.

[60] H. Sobotka, "Surface Phenomena in Chemistry and Biology," *Journal of the American Chemical Society,* vol. 81, no. 15, pp. 4122-4122, 1959.

[61] Z. Wang, F. C. Wang, and Y. P. Zhao, "Tap dance of a water droplet," *Proceedings of the Royal Society A: Mathematical, Physical and Engineering Sciences,* vol. 468, no. 2145, pp. 2485-2495, 2012.

[62] C. Antonini *et al.*, "Contactless prompt tumbling rebound of drops from a sublimating slope," *Physical Review Fluids,* vol. 1, no. 1, 2016.

[63] A. Milionis, C. Antonini, S. Jung, A. Nelson, T. M. Schutzius, and D. Poulikakos, "Contactless Transport and Mixing of Liquids on Self-Sustained Sublimating Coatings," *Langmuir,* vol. 33, no. 8, pp. 1799-1809, Feb 28 2017.

[64] G. B. Footte, "The water drop rebound problem: dynamics of collision," *Journal of the Atmospheric Sciences,* vol. 32, no. 2, pp. 390-402, 1975.

[65] C. Antonini, I. Bernagozzi, S. Jung, D. Poulikakos, and M. Marengo, "Water drops dancing on ice: how sublimation leads to drop rebound," *Physical review letters,* vol. 111, no. 1, p. 014501, 2013.

[66] X. Deng, F. Schellenberger, P. Papadopoulos, D. Vollmer, and H. J. Butt, "Liquid drops impacting superamphiphobic coatings," *Langmuir,* vol. 29, no. 25, pp. 7847-7856, // 2013.

[67] T. Mao, D. C. S. Kuhn, and H. Tran, "Spread and Rebound of Liquid Droplets upon Impact on Flat Surfaces," *AIChE Journal,* vol. 43, no. 9, pp. 2169-2179, 1997.

[68] J. O. Marston, S. T. Thoroddsen, W. K. Ng, and R. B. H. Tan, "Experimental study of liquid drop impact onto a powder surface," (in English), *Powder Technology,* vol. 203, no. 2, pp. 223-236, 2010.

[69] D. Pihler-Puzović, A. Juel, and M. Heil, "The interaction between viscous fingering and wrinkling in elastic-walled Hele-Shaw cells," (in English), *Physics of Fluids,* Article vol. 26, no. 2, 2014, Art. no. 022102.

[70] M. Rein and J. P. Delplanque, "The role of air entrainment on the outcome of drop impact on a solid surface," (in English), *Acta Mechanica,* Article vol. 201, no. 1-4, pp. 105-118, 2008.

[71] J.-D. Chen, "Growth of radial viscous fingers in a Hele-Shaw cell," (in English), *Journal of Fluid Mechanics,* vol. 201, pp. 223-242, 1989.